

**Investigation of the Induced
Magnetospheric Boundary at Titan from
Langmuir Probe Observations**

Malin Westerberg

Swedish Institute of Space Physics, Uppsala

September 12, 2007

Abstract

Titan – the only satellite in our solar system known to have a substantial atmosphere composed of nitrogen – is an interesting and fascinating world in many aspects. The study of Titan and its plasma environment is one of the major objectives of the Cassini mission and the flybys performed so far have revealed that the structure of Titan’s planetary plasma is complex and dynamic.

The goal of this thesis is to improve the understanding of Titan’s interaction with the co-rotating plasma of Saturn. This will help the research community to gain knowledge about atmospheric interactions in general and to understand the evolution of Titan’s atmosphere and ionosphere.

The main focus of this study has been on the so called Induced Magnetospheric Boundary (IMB) at Titan. The IMB is the boundary between the magnetospheric plasma of Saturn and the planetary plasma of Titan. It is desired to understand how this boundary is sensitive to the orbital position.

Investigations of the location and structure of the IMB have been performed in two ways: First, a theoretical model of the ion production in Titan’s vicinity, due to photoionization and electron impact ionization, has been developed. Second, Langmuir Probe data from three Titan flybys – T8, T10 and T12 – has been analysed. The flybys took place on the ram side, in Titan’s equatorial plane, with Cassini in sunlight on the inbound and in eclipse on the outbound. Although the flybys had similar encounter geometries they occurred at different Saturn Local Time. Finally, the observations were compared with the model predictions.

From the analysis of flybys T8 and T10 it is seen that the electron number density is sensitive to the ion production in Titan’s interaction region. The higher ion production during T8, compared with T10, leads to a higher electron number density and thereby more plasma. This influences the location of the IMB, which is found further out from Titan during T8 than during T10. For T12, on the other hand, no such relation was found, which indicates a more complex and dynamic structure of the plasma in Titan’s vicinity than assumed.

For the investigated flybys, which all occurred above Titan’s exobase level, there was no significant correlation between the plasma density and the orbital position. This implies that the plasma dynamics should be included in the model for altitudes above the exobase.

The examination of the three flybys have shown that the developed theoretical model has a great potential for further investigations of Titan’s Induced Magnetospheric Boundary. The model are also being used as a tool to improve the Langmuir Probe analysis through calculations of the photoelectron current. Together with an ionospheric chemical model (developed by Karin Ågren), the ion production model will be used to estimate the electron number density in Titan’s ionosphere.

Sammanfattning

Titan – den enda månen i solsystemet som har en väsentlig kväveatmosfär – är en intressant och fascinerande värld på många sätt. Ett av de främsta målen med Cassini-projektet är att studera Titan och dess omgivande plasma. De förbiflygningar som hittills har ägt rum har visat att strukturen på Titans jonosfär är komplex och dynamisk.

Målet med denna avhandling är att förbättra förståelsen för Titans växelverkan med Saturnus magnetosfär. Detta kan hjälpa forskarvärlden att öka kunskapen om atmosfärisk påverkan generellt och att förstå utvecklingen av Titans atmosfär och jonosfär.

Studiens främsta fokus har varit på den så kallade inducerade magnetosfäriska gränsen (Induced Magnetospheric Boundary, IMB) vid Titan. Detta är gränsen mellan Saturnus magnetosfärsplasma och Titans jonosfärsplasma. Det är önskvärt att förstå hur denna gräns förändras med Titans position i sin bana runt Saturnus.

Undersökningar av läget och strukturen hos IMB har gjorts på två sätt: Först utvecklades en teoretisk modell av jonproduktionen i Titans närhet för de två dominerande processerna; fotojonisation och jonisation från kollisioner med infallande elektroner. Sedan analyserades data från Cassinis Langmuirsond från tre olika passager av Titan; T8, T10 och T12. Dessa förbiflygningar inträffade i Titans ekvatorsplan, på den sidan där Saturnus magnetosfärsplasma träffar Titan, med Cassini i solljus på ingående delen av passagen och i skugga på den utgående. Passagerna inträffade dock med Titan i olika banposition. Slutligen jämfördes observationerna med förutsägelserna från modellen.

Från analyserna av förbiflygningarna T8 och T10 kan man se att mängden elektroner är känslig för jonproduktionen i Titans närhet. Den högre jonproduktionen under T8, jämfört med T10, leder till en större mängd elektroner och därmed mer plasma. Detta påverkar läget av IMB, som hittas längre ut från Titan för T8 än för T10. För T12 kan man däremot inte hitta ett sådant beroende, vilket betyder att plasmat i Titans närhet är mer komplext och dynamiskt än förväntat.

För de undersökta passagerna, vilka alla inträffade ovanför Titans exobas, kunde man inte hitta någon signifikant korrelation mellan plasmadensiteten och banpositionen. Detta tyder på att plasmadynamiken borde tas med i modellen för höjder ovanför exobasen.

Granskningen av de tre förbiflygningarna har visat att den framtagna teoretiska modellen har stor betydelse för fortsatta undersökningar av Titans IMB. Modellen används också som ett verktyg för att förbättra analysen av data från Langmuirsonden genom beräkningar av fotoelektronströmmen. Jonproduktionsmodellen kommer att användas tillsammans med en modell för jonosfärschemin (utvecklad av Karin Ågren) för att uppskatta elektrondensiteten i Titans jonosfär.

Contents

1	Introduction	1
2	Cassini-Huygens	5
2.1	The Mission	5
2.2	Titan Flybys	6
3	Overview of Titan	9
3.1	Atmosphere and Ionosphere	10
3.2	Magnetospheric Interaction	12
3.2.1	Saturn's Magnetosphere	12
3.2.2	Induced Magnetospheric Boundary	15
3.3	Atmospheric Loss	15
4	Ionization of Titan's Atmosphere	17
4.1	The Neutral Atmosphere	17
4.1.1	The 1D Model	17
4.1.2	The 2D Model	18
4.2	Electron Impact Ionization	18
4.3	Photoionization	21
4.4	Comparison between Production Rates	24
4.5	UV Intensity	27
5	Langmuir Probe Analysis	31
5.1	Langmuir Probe Theory	31
5.2	Analyses of the flybys T8, T10 and T12	33
5.2.1	T10	33
5.2.2	T12	37
5.2.3	T8	38
5.3	Comparison between the Flybys	39
6	Conclusions	45
6.1	Scientific Results	45
6.2	Outlook	46

A	Langmuir Probe Data Processing	49
A.1	Voltage Sweep Data	49
A.1.1	SweepMap	49
A.1.2	NewSweep	50
A.2	Continuous Data	50
A.3	Data Quality Check	51
A.3.1	Spacecraft Attitude	51
A.3.2	Ram Direction	53
A.3.3	Upper Hybrid Frequency	53
A.4	Analysis and Plotting	54
A.4.1	Correction of the Sweep Density	55
A.4.2	Estimation of the High Resolution Density	57
A.4.3	Estimation of the Plasma Speed	57
A.4.4	RPWS, CAPS and MAG Data	57
A.4.5	Plotting Tools	57
B	MATLAB Routines	59
B.1	Neutral_density_1D.m	60
B.2	Neutral_density_2D.m	62
B.3	Electronic_impact_1D.m	64
B.4	Electronic_impact_2D.m	68
B.5	Photoionization_1D.m	72
B.6	Photoionization_2D.m	76
B.7	Plot_production_trajectory.m	82
	Acknowledgements	91
	Bibliography	92

Chapter 1

Introduction

Titan is the largest moon of Saturn and the second largest satellite in the solar system after Jupiter's moon Ganymede. Titan was discovered by the Dutch astronomer Christian Huygens in 1655 while he was studying Saturn and its rings. Before 1980, when the first in situ measurements took place, scientists could only make Earth-based observations of Titan, and for a long time little was known about this mysterious moon [14].

The first two encounters with Titan were made by the Voyager spacecrafts in 1980 and 1981. Since Titan's surface is hidden in a dense, photochemical haze, no detailed study of the lower atmosphere and the surface could take place at the time. Figure 1.1 shows how Titan would look like to the naked eye. Later, Titan was examined in the infrared with the Hubble Space Telescope and interesting surface features were observed [2].

Titan has been found to be an interesting and fascinating world in many aspects. Its environment and atmosphere seem to resemble the conditions on Earth before life evolved. By studying the chemical processes taking place in Titan's atmosphere it might be possible to understand how the first building blocks of the organic molecules, on which life on Earth is based, were formed. By studying the mechanisms by which Titan is losing its ionosphere, and determining the loss rate, knowledge about the evolution of atmospheres of Earth-like planets and large moons will be gained. These are some of the reasons why the Cassini spacecraft was sent to investigate the Saturnian system.

After a seven year long journey from Earth, the Cassini spacecraft entered the Saturnian system in summer 2004. In January the following year, the Huygens probe landed on Titan and sent back the first close up images of the surface. These images revealed ice blocks, drainage channels, shorelines and boundaries between raised land and flooded plains, which fascinated scientists all around the world [23].

The Cassini mission is not only designed for studying Saturn, but also to investigate its numerous moons, and Titan is one of the primary goals of



Figure 1.1: Picture of Titan taken in the visual part of the electromagnetic spectrum. Source: <http://www.astro.helsinki.fi>, September 12, 2007.

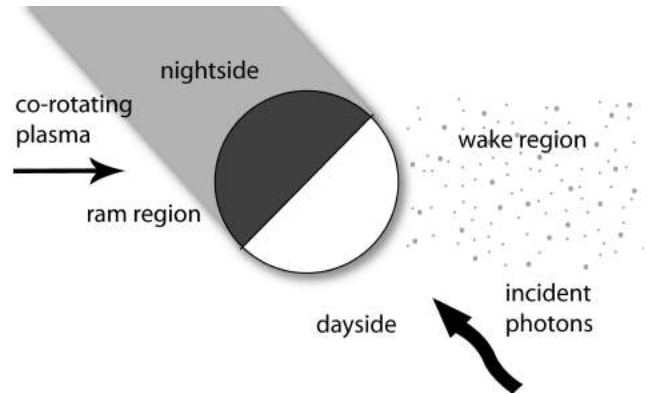


Figure 1.2: Drawing showing the different regions around Titan arising due to incident photons and electrons.

the mission. So far, the mission has been very successful and will continue to provide scientists with highly interesting data for several years.

Titan moves around Saturn at a distance of 20.3 Saturn radii. Most of the time, this is within the magnetosphere of Saturn. However, during conditions with high solar wind pressure, Titan can be found in the magnetosheath or even in the solar wind [2]. It is known that Titan possesses a dense atmosphere which interacts directly with the magnetospheric plasma of Saturn [27]. The neutral environment of Titan becomes partially ionized by solar photons, impacting electrons and through charge exchange reactions between co-rotating ions and neutral species. Cassini observations have revealed a dynamic and complex structure of the ionized environment in the vicinity of Titan.

In this report, the interaction between the co-rotating plasma of Saturn's magnetosphere and the upper atmosphere of Titan will be investigated for three flybys, by analyzing data from the Cassini Radio and Plasma Wave Science (RPWS) Langmuir Probe (LP) sensor. The study focuses on flybys that occurred on the ram side, i.e., the side of Titan facing the incoming plasma flow, see Figure 1.2. The three flybys have almost the same encounter geometry, but Titan is located at different orbital positions. The orbital position of Titan affects the relative location of the two primary ionization sources – solar EUV photons and magnetospheric electrons. The goal of this study is to understand how the location and structure of the induced magnetospheric boundary (IMB) at Titan is affected by the orbital position.

1D and 2D models of Titan's neutral atmosphere and the main ionization

sources are developed. These make it possible to plot the ionization rates along the trajectory of Cassini for the three flybys, to estimate which source of ionization is dominant and how the location of the IMB is affected by the ion production rates.

Chapter 2 briefly presents the Cassini mission and Chapter 3 provides an overview of Titan and its interesting features. In Chapter 4 the ionization model is presented and in Chapter 5 the Langmuir Probe measurements and data analyses of the different flybys are discussed. Chapter 6 contains a discussion of the results and summarizes the conclusions of this report. In Appendix A a detailed manual of how to perform Langmuir Probe data processing is provided and in Appendix B some MATLAB routines, used to develop the ionization model, are found.

Chapter 2

Cassini-Huygens

Saturn is the second largest planet in the solar system and with its spectacular ring system it might be the most beautiful. Saturn is very remote, it moves at an average distance from the Sun of 9.5 AU and it takes almost 30 years to complete one revolution. However, since Saturn is so large and reflective, it can be seen with the unaided eye as a bright star.

Saturn has a large number of moons, seven of them have diameters larger than 400 km, and Titan, which is by far the largest one, is actually a planetary world. The largest moons were probably formed at the same time as their mother planet, while the rest are tiny satellites that are either captured asteroids or collision fragments of ice and rock.

In October 1997 the Cassini spacecraft, together with the Huygens probe, started its journey to the Saturnian system to perform detailed investigations of the planet and its moons, see Figure 2.1.

2.1 The Mission

The Cassini-Huygens mission is a collaboration between NASA, ESA and the Italian Space Agency (ASI). Cassini-Huygens is one of the most ambitious missions ever launched into space. Equipped with twelve instrument packages, the spacecraft is capable of taking accurate measurements and detailed images in a variety of atmospheric conditions and light spectra. The Cassini spacecraft is the first to explore the Saturnian system from orbit, all previous explorations have been made during swift flybys.

After a seven-year journey, that included four gravity-assist maneuvers, Cassini entered into orbit around Saturn on July 1, 2004. It then began an extensive mission that will include more than 100 orbits around the planet and its moons. The main scientific objectives of Cassini include the determination of the three-dimensional structure and dynamic behaviour of the rings and the magnetosphere of Saturn as well as characterization of the surface and atmosphere of Titan.

The Huygens probe descended through Titan's atmosphere on January 14, 2005. It was designed to enter and brake in the atmosphere and parachute down to the surface while studying the content and dynamics of Titan's atmosphere. After the landing it collected data and took pictures of the surface. The first pictures that were sent back to Earth revealed that the landing site is situated close to some kind of shoreline of a liquid lake and that the surface itself appears to be clay-like. The orange landscape around the landing site is scattered with rocks and covered by a thin haze of methane. The probe continued to send data for about 90 minutes after landing.



Figure 2.1: An artist's view of Cassini in orbit around Saturn releasing Huygens. The red rectangle indicates the location of the Langmuir Probe sensor, further discussed in section 5.1. Source: <http://www.jpl.nasa.gov>, September 12, 2007.

2.2 Titan Flybys

Cassini was first planned to perform 44 Titan flybys, but since the mission has been extended until late 2010 several more flybys will take place. Each of these takes place during its own set of unique conditions. A flyby can occur on the dayside or nightside of Titan and through the wake or on the ramside. The flyby conditions are also affected by the orbital position

of Titan relative to Saturn and the Sun, and by the altitude of Cassini at closest approach. The differences between the flybys lead to a more complete picture of Titan and its atmosphere, but they also make it harder to study time-varying phenomena.

Up to the time of writing Cassini has made 36 Titan flybys. In this study, the ninth, eleventh and thirteenth flyby are analysed. These are denoted as T8, T10 and T12, respectively.¹ They all occurred on the ramside, in the equatorial plane of Titan, with Cassini in sunlight on the inbound and in eclipse on the outbound. Table 2.1 gives some parameters of the flybys.

Flyby	T8	T10	T12
Date	2005-10-28	2006-01-15	2006-03-18
Time of CA (SCET)	04:15:30	11:41:30	00:06:00
Altitude at CA [km]	1446	2041	1947
SLT	9h 20min	8h 30min	6h 25min

Table 2.1: Parameters for flyby T8, T10 and T12. SCET is the spacecraft event time. SLT is the Saturn Local Time for Titan at the time of the flyby.

¹The Titan flybys are named TA, TB, TC, T3, T4, T5 etc.

Chapter 3

Overview of Titan

Titan is the only satellite in our solar system known to have a substantial atmosphere composed of nitrogen. The second largest constituent of Titan's neutral atmosphere is methane [12]. Due to ionization of the neutrals by solar EUV photons, impacting electrons, and cosmic ray and ion precipitation, the upper parts of Titan's atmosphere is partially ionized. This upper region is called the ionosphere while the region below the ionized layer is referred to as the neutral atmosphere.

Titan and Saturn have the same orbital period, which means that the same side of Titan is always facing Saturn. All studies performed so far indicates that Titan does not possess an internal magnetic field. The solar wind and the plasma in Saturn's magnetosphere can therefore interact directly with Titan's ionosphere [18].

Titan has the same type of interaction with the ambient plasma as Mars, Venus and the comets – so called atmospheric interaction. They are all unmagnetized, or weakly magnetized, bodies possessing an ionosphere that interacts with the incoming plasma flow. In case of Mars, Venus and the comets the incident plasma is the solar wind, for Titan it is the magnetospheric plasma of Saturn. For the comets the interaction region between the incoming flow and the cometary plasma environment is very extended due to the low gravity of the bodies and the radial outflow of their atmospheres, resulting in the degas of the comet when it approaches the Sun. For Venus and Mars the corresponding interaction region is much more compressed since the gravity is higher and the ionosphere very dense [5], [6]. Titan is very interesting because it represents an intermediate case; its gravity is fairly weak but the atmosphere is yet dense and extended. In all these cases the interaction leads to atmospheric erosion through different processes, see Figure 3.4. The magnetospheric plasma of Saturn approaches Titan with a relative velocity of ~ 120 km/s. Since the incident plasma is subsonic and submagnetosonic, no bow shock is formed, in contrast to the solar wind interactions with Venus, Mars and the comets [17].

Table 3.1 gives some physical parameters of Titan [14], [28].

Radius [km]	2575
Mass [kg]	1.34×10^{23}
Average density [kgm^{-3}]	1880
Orbital period [days]	16.0
Surface temperature [K]	94
Surface pressure [kPa]	1.46
Surface gravity acceleration [ms^{-2}]	1.35
Distance from Saturn [R_S]	20.3
Mean orbital velocity [kms^{-1}]	5.57
Relative velocity of Saturn's magnetosphere [kms^{-1}]	120
Background magnetic field [nT]	5

Table 3.1: Some physical parameters of Titan.

3.1 Atmosphere and Ionosphere

About a hundred years ago, scientists started to suspect that Titan might have an atmosphere, because it is cool and massive enough to keep heavy gases. In 1944 Gerard Kuiper discovered spectral lines of methane that were reflected in sunlight from Titan, which confirmed the earlier suspicions. Today, Titan is known to be the only body in the solar system, except of the Earth, with a substantial atmosphere containing nitrogen.

Titan's atmosphere is very dense and the surface pressure is 50% higher than the surface pressure on Earth. Since the gravity on Titan is much weaker than on Earth, it means that about ten times more gas lies above a square meter of Titan's surface than above a square meter of Earth's surface. More than 90% of the atmosphere consists of molecular nitrogen (N_2), which came from the break up of ammonia (NH_3) by solar radiation in the past. Since Titan's gravity is too weak to keep the hydrogen, these atoms escaped into space while nitrogen still remains in the atmosphere. There are also a few percent of methane (CH_4) in Titan's atmosphere. The methane in the upper atmosphere interacts with the ultraviolet light from the Sun to produce hydrocarbons and other complex molecules.

The question of where Titan's atmosphere came from is still unanswered to some extent. Since ammonia is quite common in the outer solar system, it is thought that Titan's atmosphere first consisted of this compound that later on broke up into hydrogen and nitrogen as discussed above. That would explain the high content of nitrogen observed in Titan's atmosphere. The amount of observed methane is harder to explain. In the early solar system the much stronger solar wind probably compressed Saturn's magnetosphere so that Titan became exposed to the solar wind in its subsolar point much

more than today. The solar wind would then have swept away a lot of methane from Titan [2]. Since methane is also being ionized by incident photons and electrons and picked up by the magnetic field, there needs to exist some kind of source that constantly supplies new methane. This source could be impacting comets that bring methane with them to Titan, or volcanoes that supply methane from the moon's interior. Another theory is that methane became frozen in with water-ice when Titan was formed, and that this material now slowly leaks methane to the atmosphere [2].

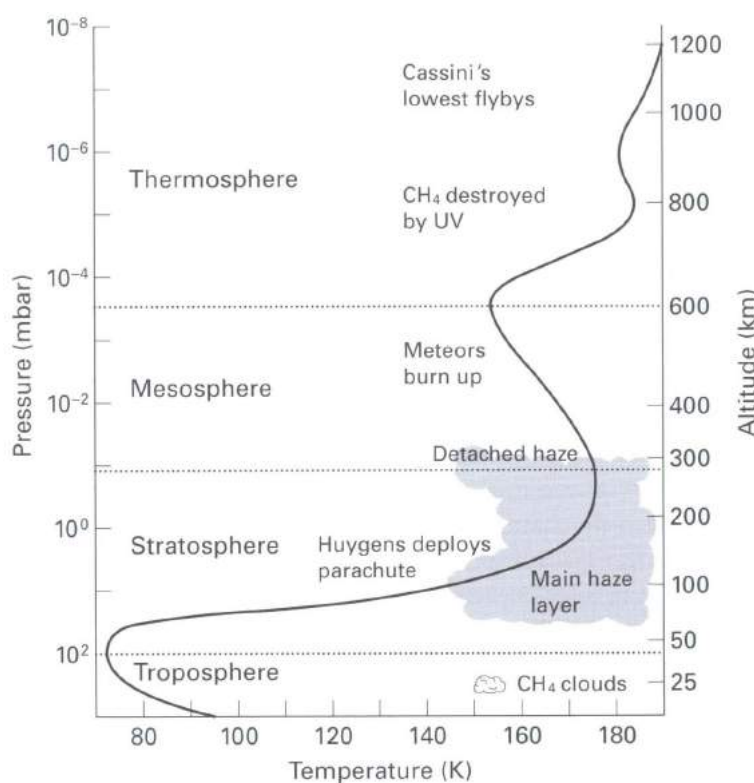


Figure 3.1: The temperature profile of Titan's atmosphere. Source: <http://www.astro.helsinki.fi>, September 12, 2007.

When looking at Titan from the outside, opaque layers of particles in the atmosphere prevent any view of the surface. Because of the low temperature, the complex molecules produced in the ionosphere condense and form a thick haze at about 100–200 km altitude. The haze prevents sunlight from penetrating down to the surface and it also gives Titan its orange-red colour. The temperature profile of Titan's atmosphere resembles that of Earth's, see figure 3.1. First, the temperature decreases with height in the troposphere after which it rises throughout the stratosphere to peak at around 175 K, which is about 80 K warmer than the surface temperature.

This warming is due to the ultraviolet radiation from the Sun and its absorption contribute to the photochemical processes in the ionosphere, excites the resulting molecules and warms the material making up the haze [13].

Solar radiation and energetic electrons in Saturn's magnetosphere ionize the upper parts of Titan's atmosphere, and an ionosphere is created. Complex photochemistry takes place in the ionosphere due to the presence of methane and solar radiation, see figure 3.2. The interaction of methane with ultraviolet radiation from the Sun produces a large number of hydrocarbons. The most dominant species in the lower atmosphere are thought to be ethane ($C_2H_6/C_2H_7^+$), ethylene ($C_2H_4/C_2H_5^+$) and acetylene ($C_2H_2/C_2H_3^+$), which can condense into droplets, fall as precipitation to Titan's surface and form liquid hydrocarbon lakes or rivers [19]. Airborne hydrocarbons also combine with nitrogen in Titan's atmosphere producing other interesting compounds, such as hydrogen cyanide (HCN/H_2CN^+). Hydrogen cyanide can join together with other molecules in long, repeating molecular chains to form so called polymers. The heavier polymer particles fall as precipitation to Titan's surface, probably covering it with a thick layer of sticky muck. Proteins are a form of polymers where different amino-acids make up the subunits in a biologically active molecular chain, but no such complex molecules are likely to be found in Titan's ionosphere due to the very cold environment far away from the Sun and the lack of oxygen. Nevertheless, some of the compounds of hydrogen, nitrogen and carbon present in Titan's atmosphere are the building blocks of the organic molecules on which life on Earth is based [14].

3.2 Magnetospheric Interaction

The internal magnetic field of Titan has been found to have a maximum strength of a 1 nT. Since this is the same order of magnitude as the magnetospheric field at Titan's orbit, the interaction between Titan and Saturn's magnetosphere is of so called atmospheric type. This means that the incident plasma interacts with the atmosphere of Titan, instead of its magnetic field, leading to the formation of an induced magnetospheric boundary (see section 3.2.2) as well as contributing to the creation of an ionosphere around Titan [27].

3.2.1 Saturn's Magnetosphere

In 1979 Pioneer 11 discovered the magnetosphere of Saturn (see figure 3.3) with its bow shock at ~ 20 Saturnian radii. The magnetic field was measured to be 600 times stronger than the magnetic field on Earth and aligned with the rotational axis of Saturn [2].

During the insertion orbit, the Cassini magnetometer (MAG) conducted in situ measurements of the magnetic field conditions of Saturn's magne-

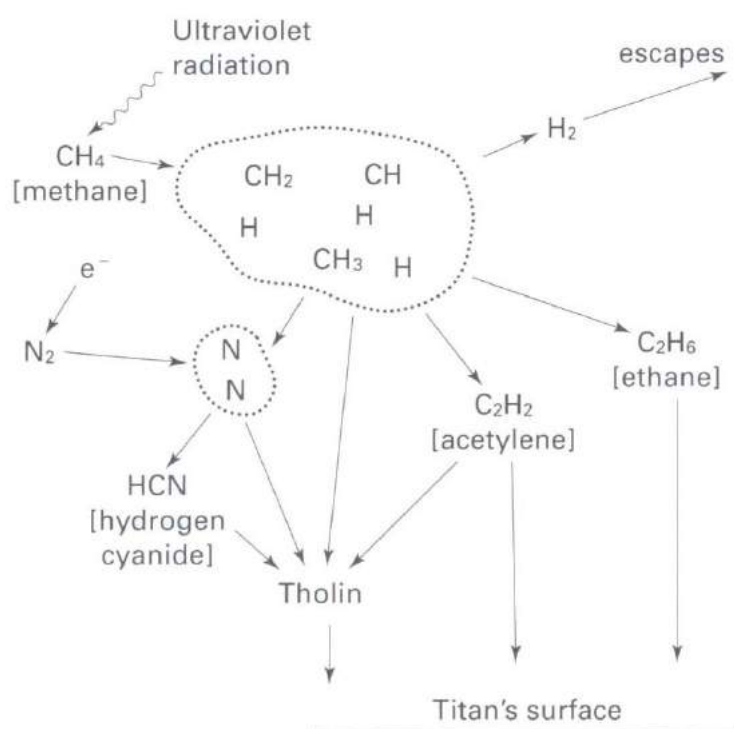


Figure 3.2: A simplified diagram of the photochemical processes taking place in Titan's ionosphere. Ultraviolet radiation from the Sun breaks methane into various fragments, called radicals (enclosed by the dotted line). Titan's gravity is too weak to keep the molecular hydrogen, which escapes to space. The radicals recombine into different organic molecules, most abundant is acetylene and ethane. These molecules can then react with other hydrocarbon and nitrogen radicals to form more complex substances. Source: <http://www.astro.helsinki.fi>, September 12, 2007.

tosphere. When the solar wind encounters the magnetic field of Saturn, with velocities up to 400 km/s, a bow shock arises. In this case the bow shock has been observed to be quasi-perpendicular, i.e., the angle between the solar wind flow and the normal to the bow shock surface is $\gg 45^\circ$ [1]. A strong bow shock, like Saturn's, converts much of the solar wind momentum flux into thermal energy of the downstream plasma. The interaction between Saturn's magnetosphere and the solar wind will be studied further throughout the Cassini mission.

It is thought that convection in the planets interior is the source of Saturn's magnetic field but exactly how the field is generated can not be explained by current theories and is now investigated by Cassini. The magnetic field lines are, to a large degree, frozen into the plasma that is confined

in the magnetosphere, i.e., to a first approximation, the magnetic field and the plasma co-rotate with the planet. The plasma thus have the same rotational period as Saturn, approximately 11 hours. The magnetospheric plasma and Titan rotate in the same direction around Saturn, but since the plasma moves much faster it hits Titan with a relative speed of ~ 120 km/s. Because of this interaction, and the incident solar radiation, Titan's upper atmosphere becomes ionized and parts of it are carried away, see section 3.3.

The magnetospheric plasma in Titan's vicinity is composed of mainly H^+ and O^+ ions [24]. The Cassini Plasma Spectrometer (CAPS) measurements obtained during the first Titan flyby confirmed the plasma characteristics from the Voyager 1 encounter [35]. The number densities and plasma temperatures of the magnetospheric protons are in the order 33% and 200 eV respectively. The corresponding numbers for the O^+ magnetospheric ions are 66% and 3 keV. The magnetospheric electron number density is approximately 0.1 cm^{-3} , but can vary by almost an order of magnitude, and the electron plasma temperature is 200 eV.

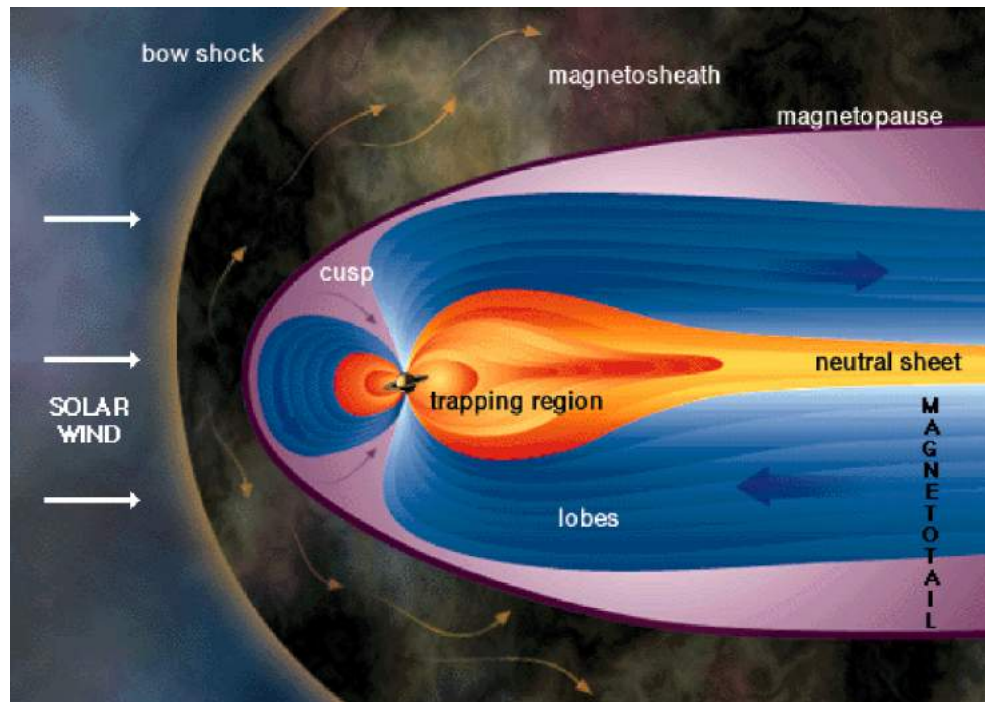


Figure 3.3: The main parts of Saturn's magnetosphere. Source: <http://www.windows.ucar.edu>, September 12, 2007.

3.2.2 Induced Magnetospheric Boundary

When the magnetospheric plasma of Saturn approaches Titan it interacts with its ionospheric plasma. Plasma originating from the ionization of the upper parts of Titan's atmosphere, is mixed with the magnetospheric plasma. This mixed plasma, the so called exospheric plasma, is mainly composed of heavy and cold ions, leading to a significant increase of the plasma density and a decrease of the plasma flow velocity. This process has been reported as mass-loading of the plasma. The cold ionosphere acts as an obstacle against the magnetospheric plasma flow and modifies and twists the field lines around Titan. Since the magnetic field lines diffuse slowly through the conductive ionosphere, this draping creates a region in the vicinity of Titan called the induced magnetosphere, see Figure 3.4. The induced magnetospheric boundary (IMB) is defined as the envelope of this induced magnetosphere, i.e., it is the boundary of Saturn's magnetosphere at Titan and it encloses the planetary plasma of Titan. The characteristics of the IMB is that the electron density increases, the plasma velocity drastically decreases and the plasma composition changes at the inbound crossing. Similar boundaries have been observed for Mars [5], [21], and Venus [6], [Sauvaud *et al.*, private communications, 2007]. Different names have been given to these boundaries, such as magnetic pileup boundary (MPB) and mass loading boundary (MLB), but they are in most aspects referring to the same phenomenon.

3.3 Atmospheric Loss

Titan's atmosphere acts as a source of both neutral gas and plasma for Saturn's outer magnetosphere. The co-rotating magnetospheric plasma outruns Titan and sweeps the upper parts of the atmosphere with it, creating an ionospheric tail in Titan's wake (see Figure 3.4). The Saturnian magnetosphere is thus important for the structure and dynamics of Titan's ionosphere. The external plasma flow and the Saturnian magnetic field induce an electric field that acts on the ions in the ionosphere. The ions are picked up by the electric field and accelerated downstream [37].

Two other processes contributing to the mass loss of the atmosphere are sputtering and loss via photochemical interactions. Sputtering takes place when energetic electrons and ions from the solar wind and the magnetosphere hit the particles in the ionosphere and cause ejection of atoms and molecules. The incident solar radiation causes ionization and dissociation of atmospheric material, so called photo-absorption (see Figure 3.2).

Usually Titan orbits within Saturn's magnetosphere but under conditions when the solar wind pressure is higher than usual, for example during increased solar activity, the magnetosphere becomes compressed. Titan can then lie outside the magnetopause during parts of its orbit, which happend

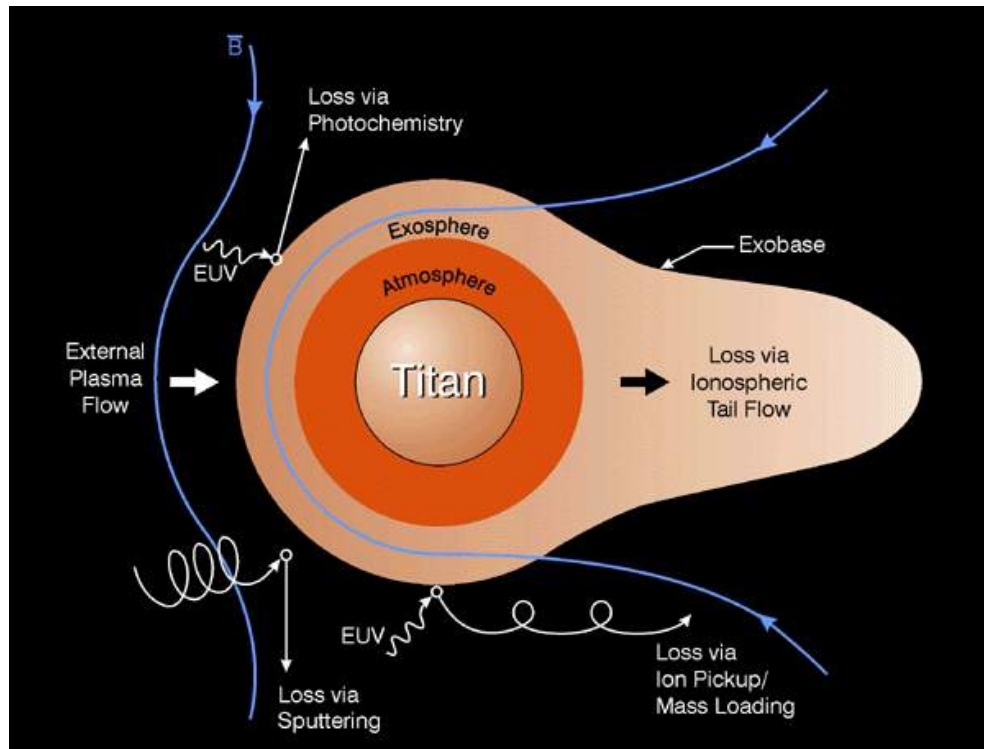


Figure 3.4: The processes by which Titan is losing its atmosphere. Source: <http://sprg.ssl.berkeley.edu>, September 12, 2007.

during flyby T32. During these conditions, the solar wind can interact directly with the ionosphere of Titan, since no magnetic field protects it. This increases the ionization rate and the atmospheric loss via sputtering, photo-absorption and ion pickup further. The total escape flux of Titan's ionosphere was recently measured by the Cassini spacecraft to 10^{25} ions per second [37].

Chapter 4

Ionization of Titan's Atmosphere

Since Titan is not protected by an intrinsic magnetic field, its atmosphere is strongly affected by the surrounding plasma flow and the solar EUV radiation. The incident high energy ions and the magnetospheric plasma of Saturn ionize Titan's atmosphere through electron impact and photoionization respectively, resulting in the formation of an ionosphere.

In this study, ion production rate models have been developed, in 1D and 2D, for N_2^+ and CH_4^+ in Titan's vicinity. The models make it possible to distinguish the main ionization process for each of the two species, and to estimate the total production rate. To determine which source of ionization that is dominant during a flyby, and how the location of the induced magnetospheric boundary may be affected by the different rates of ionization, the production along the trajectory of Cassini will be plotted.

The developed models will be used, and are already being used, in future studies. They will make it possible to calculate the electron number density and to compare the results with observations.

In this report, the two major sources of ionization are included, the electron impact and the solar EUV radiation, while the charge exchange processes are neglected. A so called transport model, that solves the equations of motion for electrons in a gas, is also omitted. The plasma transport effects become important for low electron energies and at high altitudes but is not available for this study at the time of writing [9].

4.1 The Neutral Atmosphere

4.1.1 The 1D Model

The main constituents of Titan's atmosphere are molecular nitrogen (N_2) and methane (CH_4), which together make up more than 99% of the neutrals

below the exobase level. Titan's exobase level is at 1429 km altitude ¹ and is the height above which there are negligible collisions between particles. Above the exobase level, molecular hydrogen (H₂) becomes the prominent species and production of H₂⁺ takes place far out from Titan. Since this production does not contribute significantly to the planetary plasma below 2 Titan radii, and since this study focuses on close flybys, molecular hydrogen is not included in the model.

Different atmospheric models have been developed during the last ten years [17], [36]. However, these models focus on the lower atmosphere and do not describe the atmosphere above 2000 km altitude.

Vertical density profiles were derived assuming that each neutral species is in pressure equilibrium in the gravity field of Titan,

$$\frac{dp_i}{dr} = -\frac{G M_T m_i n_i}{r^2} \quad (4.1)$$

where p_i is the pressure of species i , G is the gravitational constant, M_T is the mass of Titan, m_i is the mass and n_i the number density of species i , and r is the radial distance from the center of Titan. Together with the ideal gas law, $p_i = n_i k_B T_i$, where T_i is assumed to be constant in different temperature regions, equation 4.1 gives the number density as a function of altitude after integration,

$$n(h) = n_0 \exp\left(\frac{G M_T m_i}{k_B T_i} \left(\frac{1}{R_T + h} - \frac{1}{R_T + h_0}\right)\right) \quad (4.2)$$

where n_0 is the density at the reference altitude h_0 , R_T is the radius of Titan and h is the altitude at which the density is calculated. The temperatures and the reference densities used to compute the density profiles are given by [24], and are shown in Table 4.1. The obtained density profiles are shown in Figure 4.1.

4.1.2 The 2D Model

To develop the 2D model of Titan's atmosphere, spherical symmetry is assumed. The model gives the density of N₂ and CH₄ in a plane, e.g. the equatorial plane, as a function of the radial distance from Titan's center, see Figure 4.2.

4.2 Electron Impact Ionization

When high velocity electrons of Saturn's magnetosphere encounter the approximately stationary atmosphere of Titan, an ionization process occurs.

¹Recent measurements indicate that the exobase is located at an altitude between 1400–1600 km.

Species	Alt. [km]	Density [cm ⁻³]	Temp [K]
N ₂	700	7.2 × 10 ¹¹	171*
	1265	2.6 × 10 ⁸	149
CH ₄	925	6.1 × 10 ⁸	98*
	1265	7.0 × 10 ⁶	149

Table 4.1: The fixed densities at the reference altitudes and the different temperature regions. For altitudes between 700 km and 925 km the CH₄-density is 2.7% of the N₂-density. Values denoted by a * are estimations and are chosen to make the profiles fit between different temperature regions. The other values are given by [24]. The model is valid for altitudes larger than 700 km.

The incident electrons deposit their energy in the atmosphere by a variety of different collisions. As a result, the neutral species become excited and ionized. For a given species i , the ionization frequency is given by

$$\vartheta_i = n_e \int_{v_{min}}^{\infty} v \sigma_i^{imp}(v) f(v) 4\pi v^2 dv \quad [\text{s}^{-1}] \quad (4.3)$$

where n_e is the electron number density, σ_i^{imp} is the electron impact cross section for species i , v is the velocity and f the Maxwellian distribution function of the electron population. This ionization frequency calculation has been used to describe the production rates by electron impact in the vicinity of the comets [8]. Using the expression for the Maxwellian distribution function,

$$f(v) = \left(\frac{m_e}{2\pi k_B T_e} \right)^{\frac{3}{2}} e^{\left(-\frac{m_e v^2}{2k_B T_e} \right)}$$

and the energy of the electrons,

$$E = \frac{m_e v^2}{2}$$

equation 4.3 becomes

$$\vartheta_i = 4 n_e \left(\frac{1}{2\pi m_e} \right)^{\frac{1}{2}} (k_B T_e)^{-\frac{3}{2}} \int_{E_{min}}^{\infty} \sigma_i^{imp}(E) e^{\left(-\frac{E}{k_B T_e} \right)} E dE \quad (4.4)$$

Taking into account the energy dissipation distribution given by [29], i.e, how much energy the electrons deposit in the atmosphere at various altitudes,

$$\Lambda \left(\frac{s}{R} \right) \quad \text{with} \quad s = \int_z^{\infty} \rho(z) dz \quad \text{and} \quad R(E) = 4.30 \cdot 10^{-7} + 5.36 \cdot 10^{-6} E^{1.67}$$

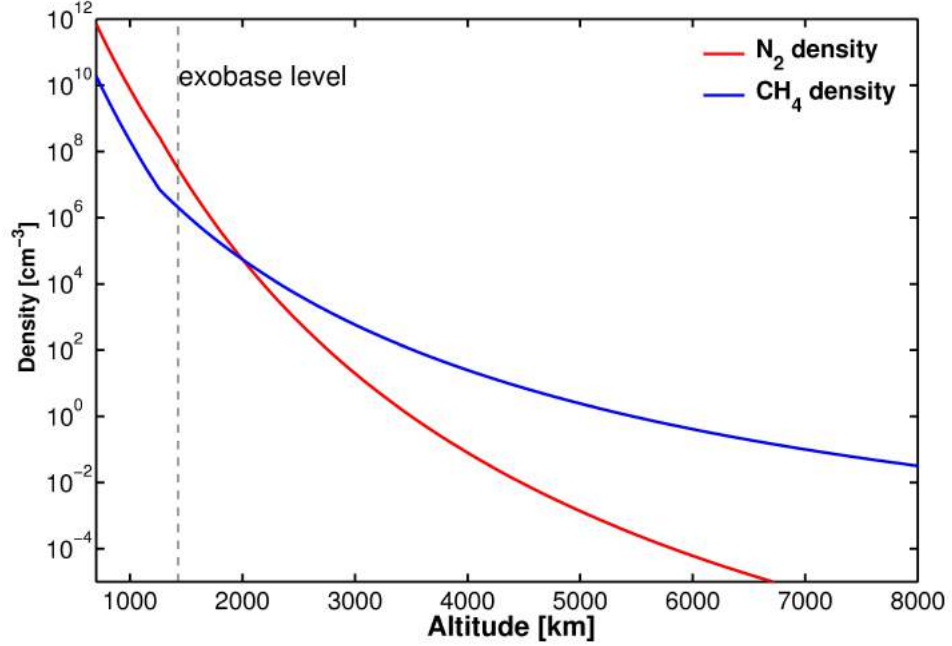


Figure 4.1: Density profiles for molecular nitrogen and methane in Titan's atmosphere.

where E is given in keV and $\Lambda\left(\frac{s}{R}\right)$ is valid for electron energies $200 \text{ eV} < E < 50 \text{ keV}$, equation 4.4 becomes

$$\vartheta_i = 4 n_e \left(\frac{1}{2\pi m_e} \right)^{\frac{1}{2}} (k_B T_e)^{-\frac{3}{2}} \cdot \int_{E_{min}}^{\infty} \sigma_i^{imp}(E) e\left(-\frac{E}{k_B T_e}\right) E \Lambda\left(\frac{s(z)}{R(E)}\right) dE \quad (4.5)$$

The production rate by electron impact is then given by multiplying equation 4.5 with the neutral density for species i , given by equation 4.2,

$$q_i(h) = n_i(h) \vartheta_i \quad [\text{cm}^{-3} \text{ s}^{-1}] \quad (4.6)$$

The production rates of N_2^+ and CH_4^+ due to electron impact were calculated assuming an electron density of $n_e = 0.1 \text{ cm}^{-3}$ and an electron temperature of $T_e = 200 \text{ eV}$ in the magnetosphere. The cross sections, $\sigma_i^{imp}(E)$, were downloaded from the National Institute of Standards and Technology database [<http://physics.nist.gov>] and the energy dissipation distribution, $\Lambda\left(\frac{s(z)}{R(E)}\right)$, was determined from [30] using the isotropic ($0^\circ - 70^\circ$) distribution. By using the calculated neutral densities, n_{N_2} and n_{CH_4} , together with equations 4.5 and 4.6, the production rates by electron impact as a

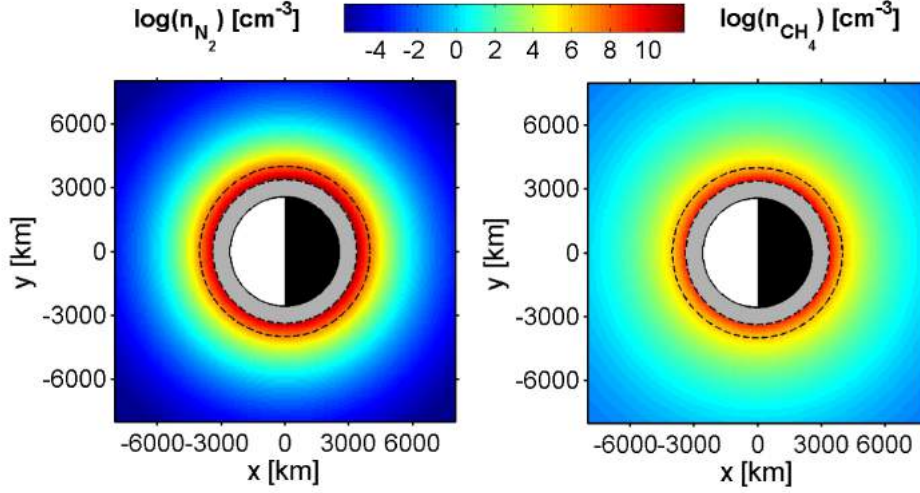


Figure 4.2: 2D density maps for N_2 (to the left) and CH_4 (to the right) in the equatorial plane of Titan. The first broken line represents the 700 km limit, which is the lower limit of the atmospheric model. Below this altitude the model gives no information about the density. The shaded area represents the region below 700 km, which is the lower limit of the atmospheric model. The second broken line represents the exobase level located at 1429 km.

function of altitude could be calculated. The results are shown in Figure 4.3 (in 1D) and Figure 4.4 (in 2D). The model discussed above only provides a first approximation of the production rate due to electron impact since the magnetic field environment around Titan is not taken into account. The electrons are assumed to be incident along a straight line, i.e., along the ideal co-rotational direction, but in reality they gyrate around the magnetic field lines.

These calculations are valid for electrons with an energy larger than 200 eV. For electrons with lower energy a transport code is mandatory.

4.3 Photoionization

Solar extreme ultraviolet (EUV) radiation is the other major source of ionization in Titan's atmosphere. When the photon flux encounters the atmosphere it is attenuated due to absorption. The decrease of the flux intensity, dI , for a travelled distance, ds_χ , assuming that the atmosphere is stratified, is given by

$$dI(s_\chi) = -I(\lambda) n(z) \sigma^{abs} ds_\chi \quad (4.7)$$

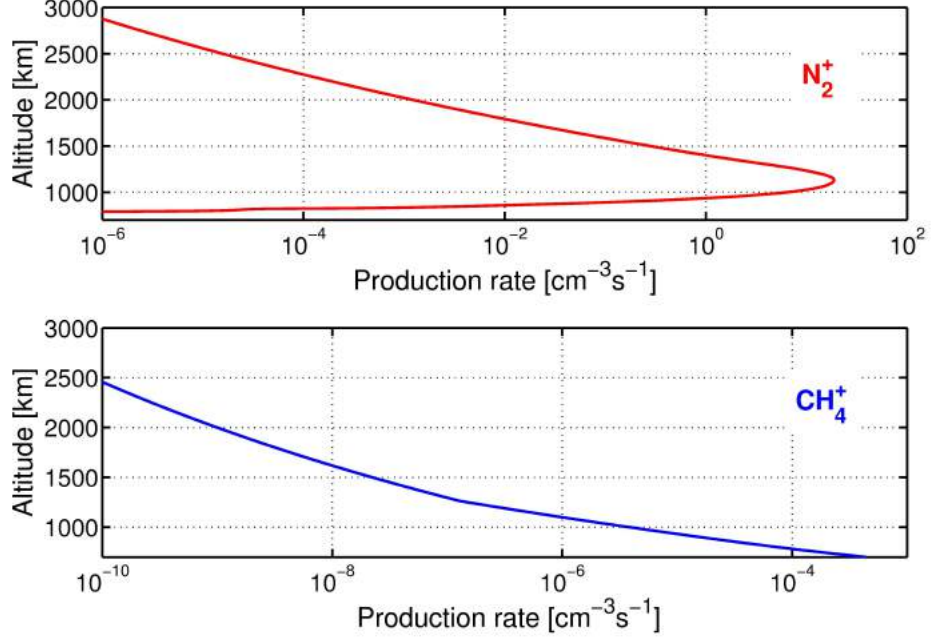


Figure 4.3: Production of N_2^+ and CH_4^+ by electron impact in Titan's ionosphere. The peak production of CH_4^+ is not seen here since it takes place below 700 km, which is the lower limit of the model.

where $n(z)$ is the neutral density as a function of altitude, σ^{abs} is the absorption cross section and ds_χ is the incremental distance given by

$$ds_\chi = -dz \sec(\chi) \quad (4.8)$$

where $\sec(\chi)$ is a function of the solar zenith angle, χ_0 , measured from the vertical [30]. On the dayside, i.e., for the case when $\chi_0 < 90^\circ$, this function is given by

$$\sec(\chi) = \left[1 - \left(\frac{R + z_0}{R + z} \right)^2 \sin^2(\chi_0) \right]^{-1/2} \quad (4.9)$$

where R is the radius of Titan, z_0 is the altitude at which the photon flux is evaluated and z is the integration path from z_0 towards the Sun along the optical path. For the case when $\chi_0 \leq 75^\circ$, $\sec(\chi) \approx \sec(\chi_0)$ for values of z_0 corresponding to ionospheric altitudes.

Substituting equations 4.8 and 4.9 into equation 4.7 and integrating gives the photon flux intensity as a function of altitude, wavelength and solar zenith angle,

$$I(z, \lambda, \chi) = I_\infty \exp \left[- \int_\infty^z \sum_i n_i(z) \sigma_i^{abs}(\lambda) \sec(\chi) dz \right] \quad (4.10)$$

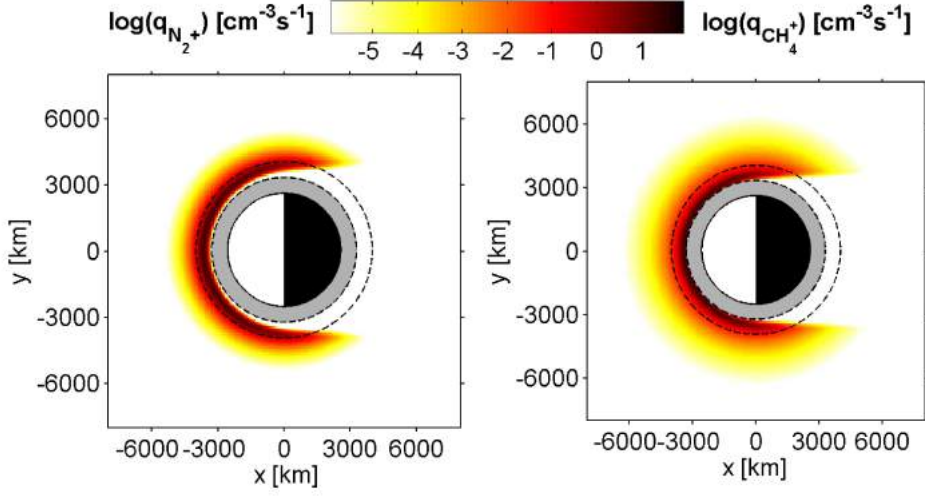


Figure 4.4: 2D map of the electron impact ionization rates for N_2^+ (to the left) and CH_4^+ (to the right) in the equatorial plane of Titan. The electrons are incident from the $-x$ direction and the photons from the direction given by SLT for flyby T10, see table 2.1. The first broken line represents the 700 km limit, which is the lower limit of the atmospheric model. Below this altitude the model gives no information about the density. The second broken line represents the exobase level located at 1429 km.

where I_∞ is the non-attenuated solar flux, i is the notation of the absorbing species and the integration is to be carried out along the optical path. The argument of the exponential in equation 4.10 is defined as the optical depth,

$$\tau(z, \lambda, \chi) = \int_\infty^z \sum_i n_i(z) \sigma_i^{abs}(\lambda) \sec(\chi) dz \quad (4.11)$$

On the nightside, i.e., for the case when $\chi_0 > 90^\circ$, the optical depth is given by

$$\begin{aligned} \tau(z, \lambda, \chi) = & 2 \int_\infty^z \sum_i n_i(z) \sigma_i^{abs}(\lambda) \left[1 - \left(\frac{R + y_\perp}{R + z} \right)^2 \right]^{-1/2} dz \\ & - \int_\infty^z \sum_i n_i(z) \sigma_i^{abs}(\lambda) \left[1 - \left(\frac{R + z_0}{R + z} \right)^2 \sin^2(\chi_0) \right]^{-1/2} dz \end{aligned} \quad (4.12)$$

where y_\perp is the distance in the y -direction from Titan's surface to z_0 .

The photoionization rate for species i can be written as

$$P_i(z, \chi) = n_i(z) \int_0^{\lambda_\infty} I_\infty e^{[-\tau(z, \lambda, \chi)]} \sigma_i^{ph}(\lambda) d\lambda \quad (4.13)$$

where $\sigma_i^{ph}(\lambda)$ is the photoionization cross section as a function of wavelength [30].

The production rates of N_2^+ and CH_4^+ due to photoionization were calculated using the neutral densities, n_{N_2} and n_{CH_4} , together with equations 4.7 – 4.13. The results are shown in Figure 4.5 (in 1D, along the vertical towards the Sun) and Figure 4.6 (in 2D). The cross sections, σ_i^{abs} and σ_i^{ph} , were given by [32] for wavelengths in the range $50 \text{ \AA} < \lambda < 1050 \text{ \AA}$. The non-attenuated solar flux, I_∞ , was also given by [32] for the same wavelength range based on the EUVAC solar flux model, which accounts for solar activity variations. In the 1D model the photons are assumed to be incident along the vertical, giving $\chi \equiv 1$. In the 2D model the solar zenith angle needs to be calculated for each point where the ionization rates are calculated [30].

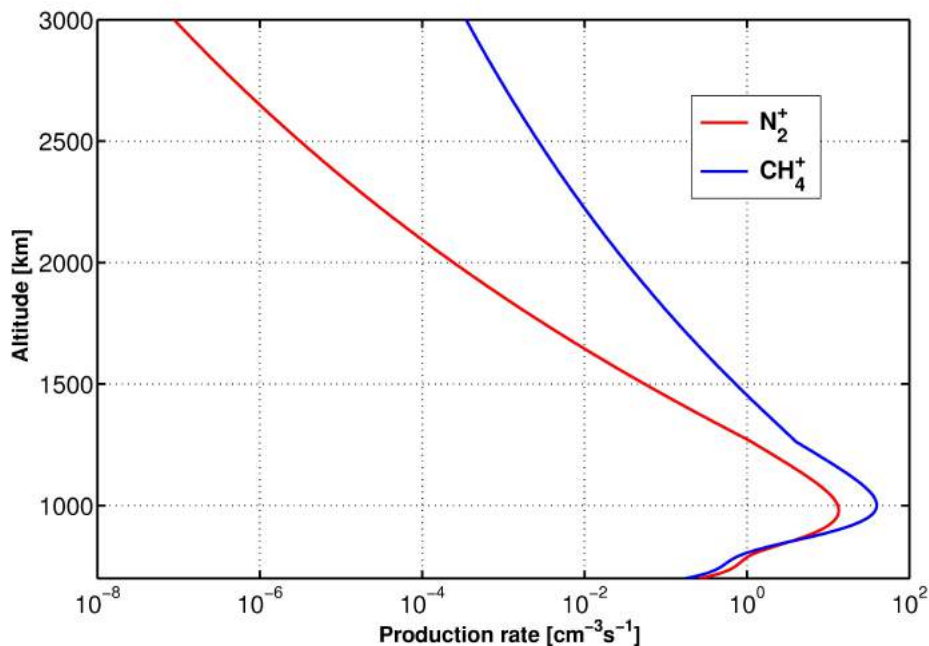


Figure 4.5: Production of N_2^+ and CH_4^+ by photoionization along the incident path of the photons.

4.4 Comparison between Production Rates

The models described in this chapter can be used as a tool to investigate the relative importance of the two different ionization sources for a given orbital position of Titan. Picture 4.7 shows the phases of Titan in its orbit around Saturn. It takes 16 days for Titan to perform one orbit, while the mag-

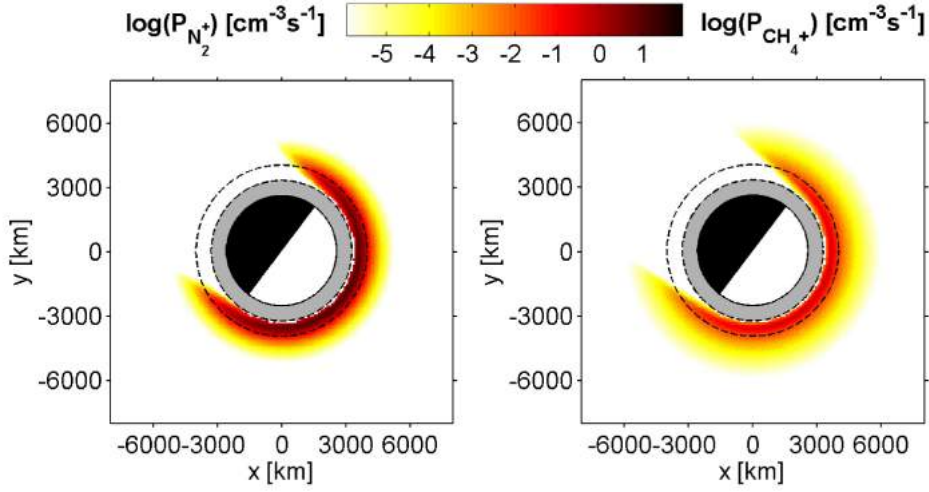


Figure 4.6: 2D map of the photoionization rates for N_2^+ (to the left) and CH_4^+ (to the right) in the equatorial plane of Titan. The electrons are incident from the $-x$ direction and the photons from the direction given by SLT for flyby T10, see table 2.1. The first broken line represents the 700 km limit, which is the lower limit of the atmospheric model. Below this altitude the model gives no information about the density. The second broken line represents the exobase level located at 1429 km.

netosphere of Saturn revolves in ~ 11 hours. The solar radiation is always incident from the same direction while the direction of the magnetospheric electrons depends on the orbital position of Titan. When Titan is located at 18 Saturn Local Time (SLT) the two ionization sources are on the same side of Titan, while they are on opposite sides at 6 SLT. 12 SLT and 24 SLT represent intermediate cases.

The three flybys investigated in this study – T8, T10 and T12 – all occurred on the ram side in the equatorial plane of Titan, with Cassini in sunlight on the inbound and in shadow on the outbound, see Figure 4.8. This implies that the electron impact ionization is dominant on the outbound since the spacecraft is in eclipse. For the inbound part of the flyby more work is required to find out which source of ionization that is the most important one. In the region where ionization from both sources occurs, the contribution for each source needs to be calculated separately to determine the dominant ionization process. Figure 4.8 illustrates this problem and shows the region where both ionization processes are taking place.

To analyse this problem, the different production rates derived in section 4.2 and 4.3 have been used to calculate the production along the trajectory of Cassini for each of the three flybys. Figure 4.9 shows the production of N_2^+ during the T10 flyby. It is seen that electron impact is the dominant

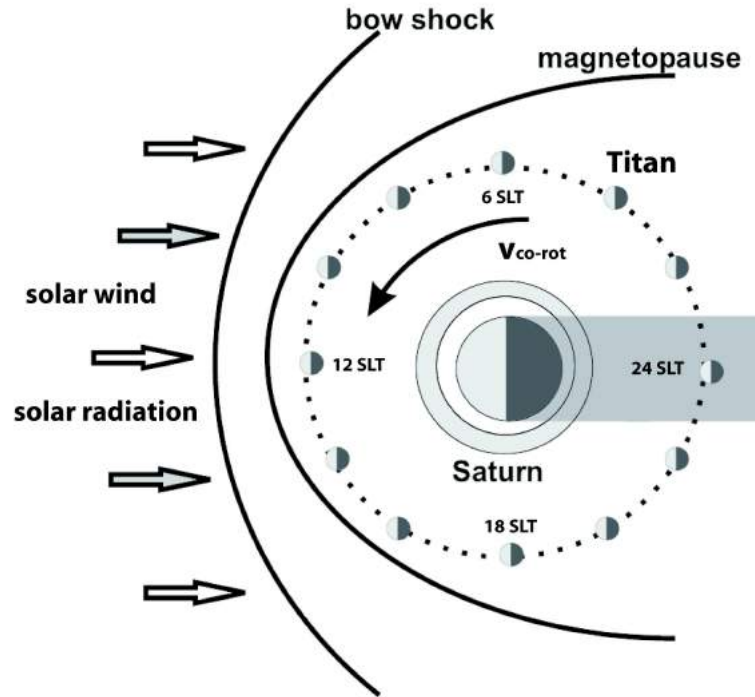


Figure 4.7: Schematic showing Titan's orbital phases around Saturn. The magnetospheric plasma of Saturn co-rotates with the planet and fall in on Titan with a relative velocity of ~ 120 km/h.

source of ionization by almost a factor 10 on the inbound. On the outbound the photoionization drops to zero since the spacecraft enters the nightside of Titan. For a more detailed comparison between the production rates for the investigated flybys, see section 5.3.

The derived photoionization models will be used in future studies by Karin Ågren at the Swedish Institute of Space Physics. The Ion and Neutral Mass Spectrometer (INMS) onboard Cassini provides the neutral density in Titan's atmosphere for the five species N_2 , CH_4 , HCN , C_2H_4 and HC_3N . The N_2 -density will be used as input in the electron impact ionization model from section 4.2 together with a transport code for the behaviour of the low energy electrons. The obtained production rate, together with the production rate from the photoionization model in section 4.3, will be the input in a chemical model where the ion density profiles in Titan's ionosphere are determined. Assuming quasi-neutrality, i.e., $\sum_i n_i = n_e$, will make calculations of the electron number density possible. The result can then be directly compared with Langmuir Probe data.

The 2D models can provide the production rates of N_2^+ and CH_4^+ along the trajectory of Cassini for any flyby with similar encounter geometry as

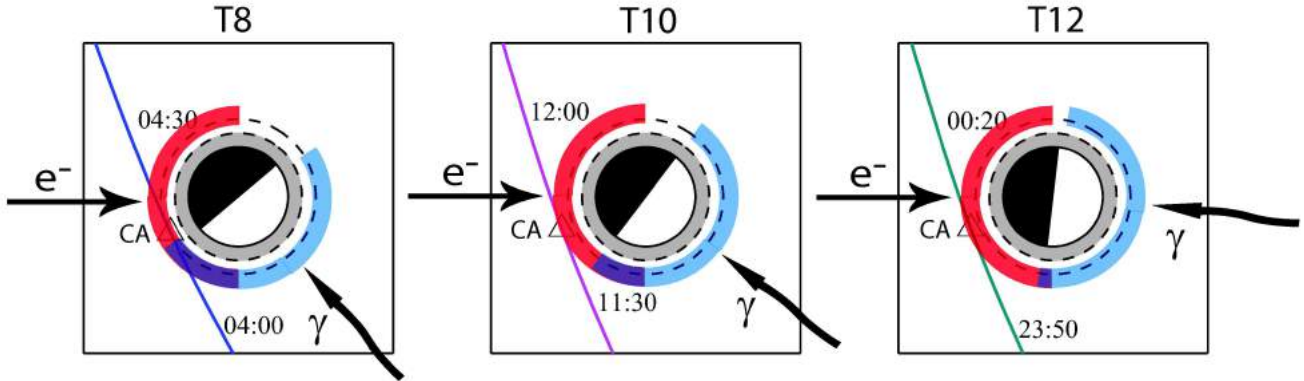


Figure 4.8: Schematic showing the location of the two major ionization sources for the investigated flybys – electron impact ionization (red) and photoionization (blue). The angle between the incident electrons and photons are changing with the orbital position of Titan and determines the region where both ionization processes occurs (purple). This region requires more detailed studies to determine which source of ionization that dominates.

the flybys investigated in this study. The models have also been extended into 3D and can now be used to investigate *any* flyby.

4.5 UV Intensity

The photoionization model in section 4.3 provides the solar photon flux as a function of altitude, wavelength and solar zenith angle, $I(z, \lambda, \chi)$. This UV intensity, also denoted Φ_λ , can then be used together with the photoelectron yield function, Y_λ , given by [39], to obtain the photoelectron current to the Langmuir Probe,

$$I_{pe} = A_c e \int_0^{\lambda_\infty} \Phi_\lambda Y_\lambda d\lambda \quad (4.14)$$

where A_c is the area of the photon collector viewed from the Sun and e is the electron charge. Since no investigations on the LP response to solar radiation have been made for the LP on Cassini, the same yield is being used as for the probes on Pioneer 11, see [7]. These probes were made of molybdenum and rhenium, while the LP on Cassini is in titanium. The Ly- α radiation is not included here – since no absorption cross sections has been found for wavelengths above 1050 Å- which might affect the photoelectron current slightly.

The LP measures the *total* current, i.e., the sum of the electron, ion and photoelectron currents. For negative bias voltages, the electron current can be neglected and the ion current, with the photoelectron contribution,

is measured. When the photoelectron current is known explicitly, improvements of the data analysis can be made. For example, it will be possible to obtain a better estimation of the ion ram speed from the ion current, see section A.4.3.

The solar photon flux can be integrated over all wavelengths and plotted along the trajectory of Cassini to obtain an estimation of the total UV intensity during a flyby, see Figure 4.10.

Equation 4.14 has been used to obtain Figure 4.11. This figure shows the photoelectron current as a function of wavelength in the non-attenuated solar flux region as well as in the absorption region close to Titan. The solar UV flux is attenuated by the molecules in Titan's atmosphere, which results in a wavelength dependent decrease of the photoelectron current, see Figure 4.11.

The photoelectron current to the Langmuir Probe has also been determined along the trajectory of Cassini for the T10 flyby, see Figure 4.12.

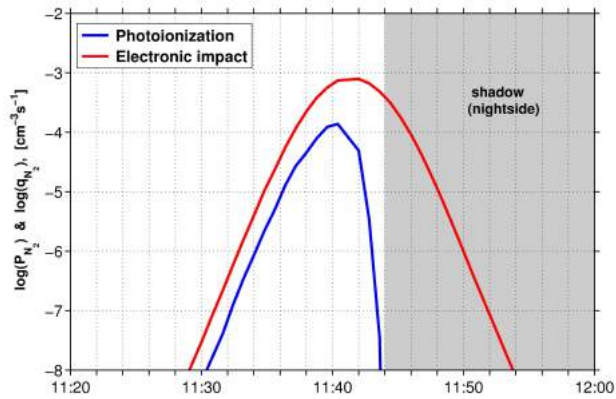


Figure 4.9: Production of N_2^+ due to electron impact ionization and photoionization along the trajectory of Cassini during T10.

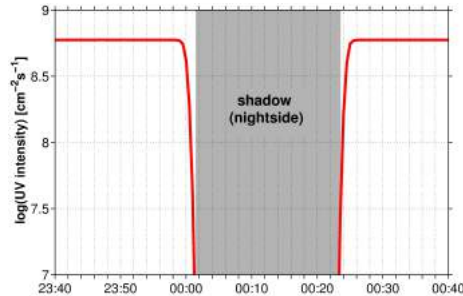


Figure 4.10: Total UV intensity along the trajectory of Cassini during flyby T12.

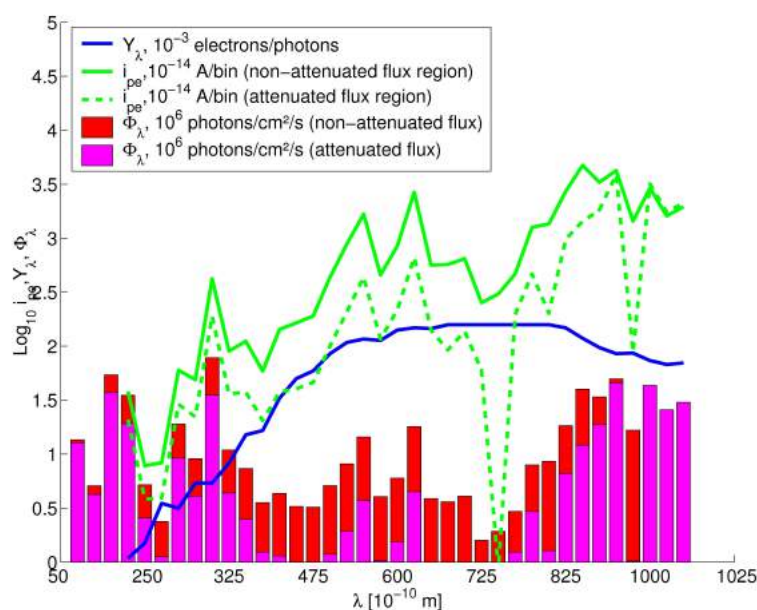


Figure 4.11: Solar photon flux (non-attenuated; at 11:21 SCET (red) and attenuated; at 11:41 SCET (magenta)), photoelectron yield function (blue curve) and photoelectron current with attenuated (dashed green curve) and non-attenuated (solid green curve) solar flux, as a function of wavelength for flyby T10.

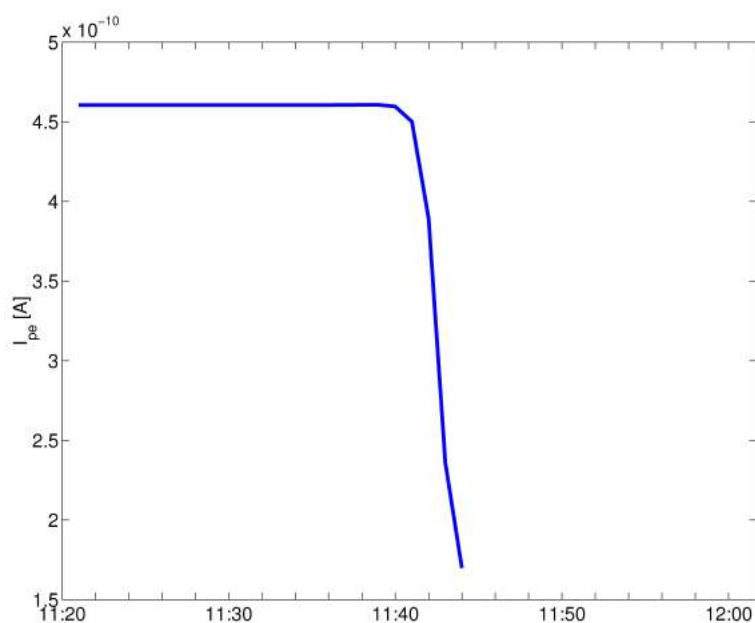


Figure 4.12: Photoelectron current along the trajectory of Cassini during flyby T10.

Chapter 5

Langmuir Probe Analysis

Cassini is equipped with twelve different science instrument packages, all designed to carry out various scientific measurements in the Saturnian system. The instrument with the greatest relevance for this study is the Langmuir Probe (LP), which is a part of the Radio and Plasma Wave Science (RPWS) package. The Langmuir Probe onboard Cassini was designed and built at the Swedish Institute of Space Physics in Uppsala (IRFU). It consists of a titanium sphere, with a diameter of about 50 mm, placed on a 1.5 m long boom, see Figure 5.1. With the Langmuir Probe, the density and temperature of the surrounding plasma can be determined, and sometimes also the spacecraft potential, plasma flow speed and mean ion mass.



Figure 5.1: A Langmuir Probe. Source: <http://www.space.irfu.se>, September 12, 2007.

5.1 Langmuir Probe Theory

The basic principle for measuring plasma parameters with a Langmuir Probe is to insert the probe into a plasma and apply a potential to the probe, which then will be charged. If the probe is positively charged, it will attract mainly free electrons from the plasma. As a result, a current will flow from the spacecraft to the probe in proportion to the density of the surrounding plasma. If the probe is instead negatively charged, the resulting current will

consist mainly of ions from the plasma and photoelectrons from the probe itself.

From Orbital Motion Limited (OML) theory [11] for a spherical probe with a positive bias voltage, $U_B > 0$, the electron current, I_e , and the ion current, I_i , in a stationary plasma can be written

$$I_e = I_{e0} (1 - \chi_e U_B) \quad (5.1a)$$

$$I_i = I_{i0} e^{-\chi_i U_B} \quad (5.1b)$$

and for the case with a negative bias voltage, $U_B < 0$, the currents are given by

$$I_e = I_{e0} e^{-\chi_e U_B} \quad (5.2a)$$

$$I_i = I_{i0} (1 - \chi_i U_B) \quad (+I_{pe}) \quad (5.2b)$$

where I_{pe} is the current due to the photoelectrons, see section 4.5, and

$$I_{e0} = -A_{LP} n_e q_e \sqrt{\frac{k_B T_e}{2\pi m_e}} \quad (5.3a)$$

$$I_{i0} = -A_{LP} n_i q_i \sqrt{\frac{v_i^2}{16} + \frac{k_B T_i}{2\pi m_i}} \quad (5.3b)$$

and

$$\chi_e = \frac{q_e}{k_B T_e} \quad (5.4a)$$

$$\chi_i = \frac{q_i}{\frac{m_i v_i^2}{2} + k_B T_e} \quad (5.4b)$$

where A_{LP} is the surface area of the Langmuir Probe. From equations 5.3 – 5.4 it is possible to determine the electron number density and temperature, n_e and T_e , the ion velocity and temperature, v_i and T_i , and the mean ion mass, m_i , for a given probe current.

The Langmuir Probe always measures the total current, i.e., the sum of the electron and ion currents,

$$I = I_e + I_i \quad (5.5)$$

which is dependent on the bias voltage, U_B . The two modes of operation used for the Langmuir Probe onboard Cassini are called sweep mode and continuous mode. In the sweep mode, the bias voltage of the probe is varied over an interval, usually from -32 V to $+32$ V, while the current is measured. The relationship between the bias voltage and the probe current can

be displayed in a so called U-I curve, see Figure 5.2, from which the plasma parameters in equations 5.1 – 5.4 can be derived. For large positive bias voltages the electron current will be dominant and the relationship will be linear. For large negative bias voltages, on the other hand, it is the ion current that is dominant. Analyses of the voltage-current (U-I) characteristic provide all the information needed to extract the plasma parameters from the LP measurements.

Between the sweeps, the LP is working in its continuous mode; the bias voltage is fixed at a constant value, usually +10 V, and the current is sampled at 20 Hz. Since the bias voltage is positive, it is mainly the electron current that is measured.

Using the information provided by the sweep analysis, and assuming that the electron temperature and spacecraft potential do not alter significantly between two sweeps, a high temporal resolution of the electron number density can be obtained, see section A.2.

5.2 Analyses of the flybys T8, T10 and T12

In order to analyse the Langmuir Probe measurements, the collected data needs to be prepared in a series of steps. To start with, the LP data needs to be calibrated and fitted to theoretical expressions. Data quality checks needs to be performed and the data should then be prepared for plotting.

These steps have been carried out for the flybys T8, T10 and T12 and are explained in detail in Appendix A.

5.2.1 T10

Figure 5.3 shows the trajectory of Cassini during the T10 flyby, which occurred in the equatorial plane of Titan on January 15, 2006. The flyby took place on the ramside, i.e., on the side facing the incoming co-rotational plasma, see Figure 1.2 in chapter 1, with closest approach at 11:41 SCET¹ at an altitude of 2041 km. Cassini crossed the inbound IMB sometime between 11:31 SCET and 11:33 SCET, and the outbound IMB between 11:45 SCET and 11:47 SCET, and thus spent ~15 minutes in the Titan interaction region. To emphasize the location of the inbound and outbound induced magnetospheric boundary, the electron number density is projected along the trajectory. The IMB is defined in section 3.2.2.

Figure 5.4 gives an overview of the data from the T10 flyby. The CAPS ion spectrogram in panel a) does not give any valuable information since the ion beam spectrometer was not pointing in the direction of the incoming plasma during the flyby. The CAPS electron spectrometer, on the other

¹Spacecraft Event Time

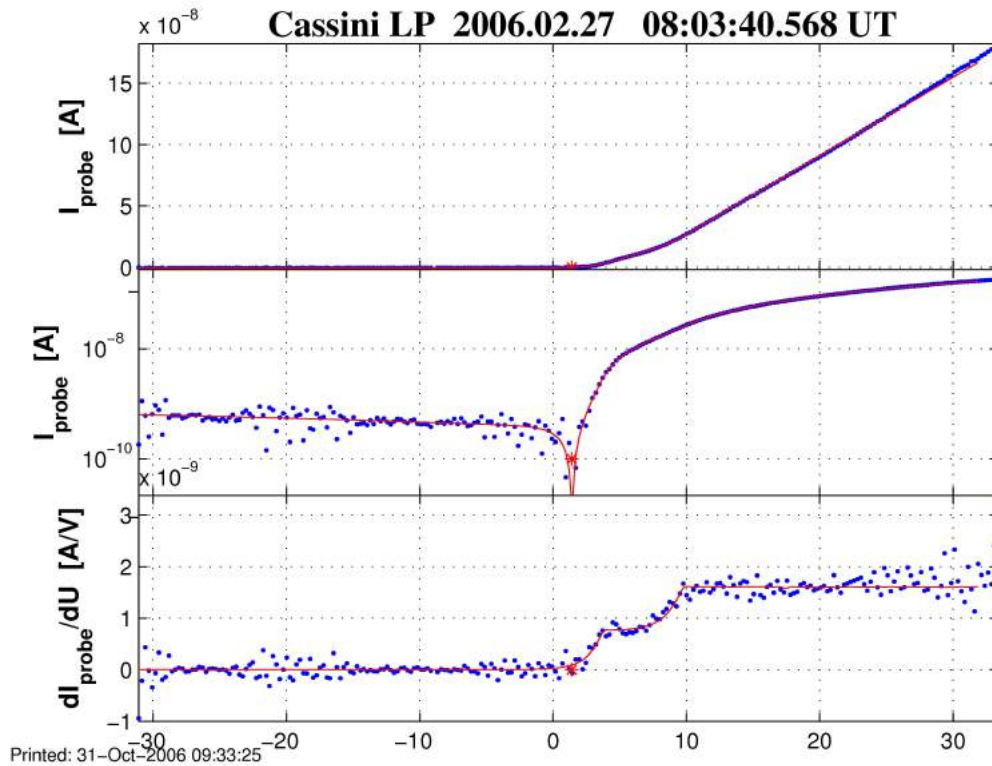


Figure 5.2: Typical U - I characteristic from a Langmuir Probe sweep in the close vicinity of Titan. The figure shows the magnitude of the collected current in both linear scale (upper panel) and logarithmic scale (middle panel). The current gradient, $\frac{dI}{dU}$, is also shown (lower panel). The blue points represent real data points while the solid line is a fit of these points to the theoretical expressions given by equations 5.1 – 5.4.

hand, can be used to estimate the electron number density and temperature with help of a one-dimensional Maxwellian fit method. Although these measurements are not as accurate for cold plasma as those given by the Langmuir Probe, they are a good complement to the LP data. The electron spectrogram in panel b) shows a band of electrons with energies around 200 eV, which is the typical energy of the electrons in Saturn's magnetospheric plasma. The high energy electrons (clearly seen on the inbound between 11:00 SCET and 11:25 SCET) are probably a mixture of magnetospheric plasma and a cold, unknown component. This structure also gives a signature in the LP data (see panel f). The magnetic field variations in the MAG data in panel e) are also associated with these high energy electrons. Low energy electrons (<5 eV) are not visible after the outbound IMB since

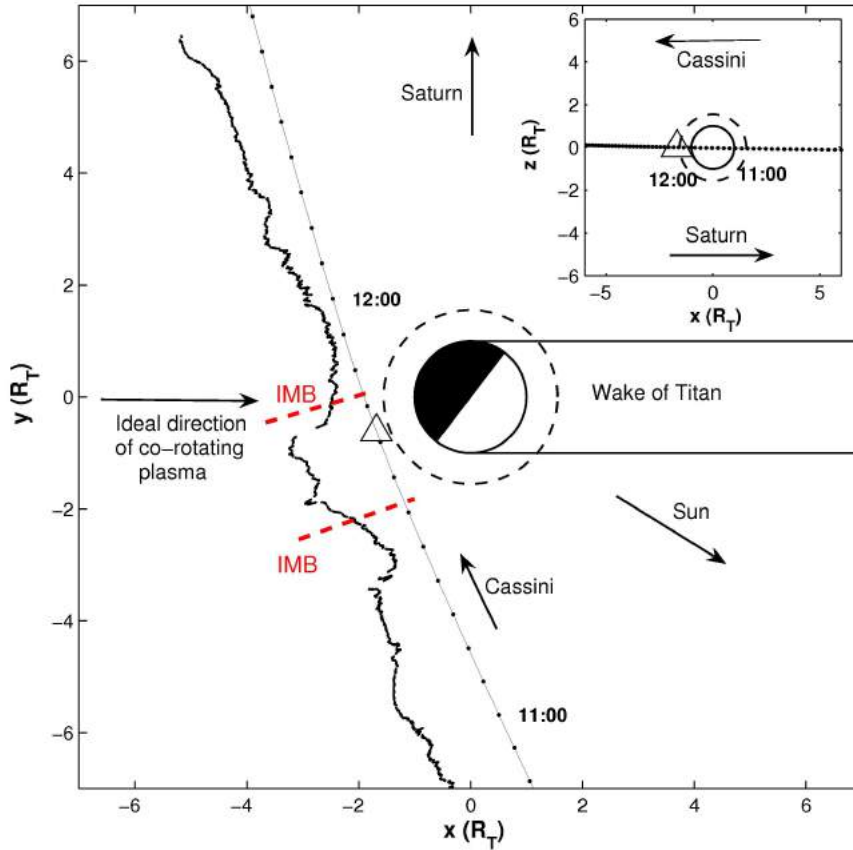


Figure 5.3: The T10 flyby trajectory in the Titan centered coordinate system. Tickmarks are displayed every 5th minute and the electron number density is projected along the trajectory.

the instrument is then in eclipse and no photoelectrons are produced.

Panel c) shows the RPWS high frequency wave intensities with the upper hybrid line emphasized in the Titan interaction region. Panel d) presents the calibrated LP measurements; negative bias voltage gives the ion current and positive bias voltage the electron current.

In the following, the Titan interaction region, which starts and ends with the crossings of the induced magnetospheric boundary, will be in focus. Panel f) shows that the magnetospheric electron number density is $\sim 0.1 \text{ cm}^{-3}$, while the corresponding density in the Titan interaction region is a few cm^{-3} .

Figure 5.5 gives a closer and more complete view of the Langmuir Probe observations from the T10 flyby. Panel b) presents the electron number density from the sweep analysis (red points), from the continuous data (blue line) and from the upper hybrid resonance emissions (black line, see section

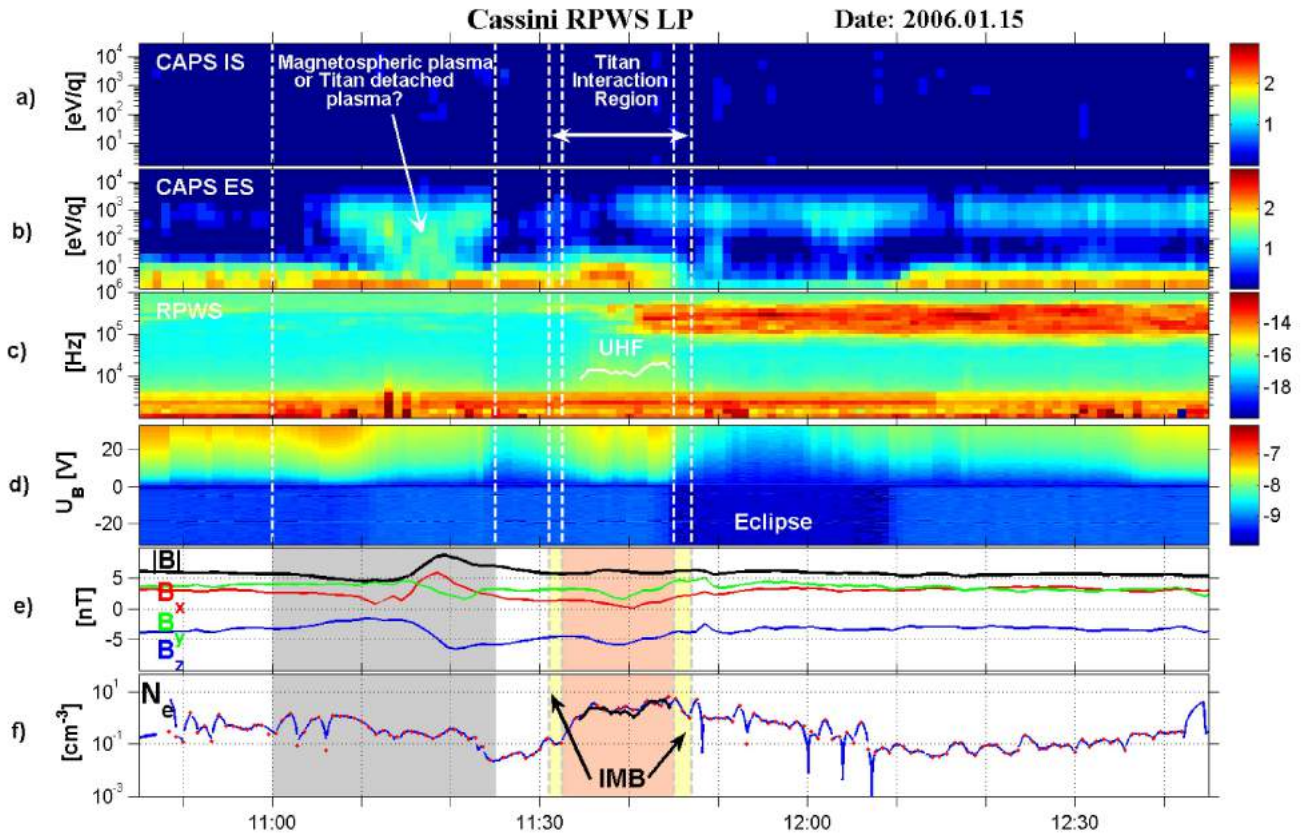


Figure 5.4: CAPS, RPWS, MAG and LP observations during the T10 flyby. Panels a) and b) are the CAPS ion spectrogram and electron spectrogram, respectively. Panel c) shows the RPWS high frequency wave intensities with the upper hybrid line emphasized. Panel d) gives the calibrated LP observations, and the magnetic field data are shown in panel e). Panel f) presents the electron number density derived from the sweep analysis (red points) and the continuous data (blue curve). The density deduced from the upper hybrid resonance emissions is also shown (black curve). The three top panels have a time resolution of one minute.

A.3.3). It is seen that the LP density is in good agreement with the density of the upper hybrid line.

Panel c) shows the electron temperature, which is ~ 1 eV in the Titan interaction region. Outside of this region the LP does not provide accurate measurements of the temperature. The magnetospheric electron temperature is ~ 200 eV and the LP is designed for cold and dense plasma. Estimations of the electron temperature from the CAPS electron spectrometer are more trustful in the magnetosphere of Saturn.

Panel d) shows the spacecraft potential, which is positive in the magnetospheric plasma and negative in the Titan interaction region. Since the electrons have higher velocities than the ions, and since the electron number density is higher in the Titan interaction region than in the magnetosphere, more electrons hit the spacecraft inside the IMB. This causes in a negative charge on the spacecraft in the cold plasma close to Titan, and is the reason why $U_{SC} < 0$ there.

Panel e) gives estimations of the ion ram speed using two different methods. Assuming that the kinetic energy (the ram term) dominates over the thermal energy, i.e., $k_B T_i \ll \frac{m_i v_i^2}{2}$, either the DC level of the ion current or the slope of the ion current can be used to determine the ram speed, see equations 5.1 – 5.4. When using the DC level of the ion current (black curve) quasi-neutrality is assumed, i.e., $\sum_i n_i = n_e$. The ram speed is calculated for two different ion masses – light ions ($m_i = 1$, red curve) and heavy ions ($m_i = 28$, blue curve). The ion ram speed given by the slope of the ion current (black curve) is seen to drop from ~ 100 km/s in the magnetosphere to ~ 10 – 50 km/s in Titan’s interaction region. The spacecraft speed was ~ 6 km/s during the flyby (green line).

The inbound crossing of the IMB indicates the transition from Saturn’s magnetospheric plasma to the planetary plasma of Titan. An increase in electron number density, a decrease in ion ram speed and a change in ion composition are the criterias used to locate the induced magnetospheric boundary, see section 3.2.2. It is clearly seen in panel b) and e) of Figure 5.5 that the density increases and the ion speed decreases at the estimated location of the inbound IMB. The ion ram speed calculated from the slope of the ion current coincides with the speed calculated using $m_i = 1$ *outside* the IMB and with the speed calculated using $m_i = 28$ *inside* the IMB, thus suggesting a change in ion composition at the IMB. The location of the outbound IMB is not as clearly defined as the inbound since the LP is then in eclipse, a case for which the LP analysis needs to be improved.

In order to get a more precise location of the IMB, further studies need to be performed. More investigations are also needed to get a more accurate estimation of the ion ram speed. The ion speed presented here is only a first order approximation since it is a derived parameter, not a measured one, and since the magnetospheric plasma speed is as high as 120 km/s close to Titan. With a better estimation of the photoelectron current, the accuracy of the speed estimation will also be improved. A method to calculate the photoelectron current is given in section 4.5.

5.2.2 T12

The T12 flyby occurred on Mars 18, 2006, with closest approach at 00:06 SCET at an altitude of 1947 km. The encounter geometry was similar to the one for the T10 flyby, see Figure 5.8. Figure 5.6 shows the result of the T12

analysis with the estimated locations of the IMB.

During the flyby, the electron number density was $\gtrsim 10 \text{ cm}^{-3}$ and the temperature $0.5 - 2 \text{ eV}$ in the interaction region, as seen in panels b) and c). As expected, the spacecraft potential became negative – meaning that the LP encountered a cold plasma population, the ion speed decreased ($350 \text{ km/s} \rightarrow 30 \text{ km/s}$) and there was a change in ion composition, at the crossing of the inbound IMB, see panels d) and e).

At the inbound IMB, between 23:47 SCET and 23:53 SCET, there is a discrepancy between the LP density and the density derived from the upper hybrid line by a factor 10. It is known that the photoelectron contribution is sensitive to the spacecraft attitude, see [20], and one possible explanation of this deviation is that the spacecraft attitude also influences the estimation of the spacecraft potential, which is used to determine the electron number density. Further investigations on this subject are in progress. It should also be kept in mind that the LP is designed to be used in cold and dense ($n_e < 5 \text{ cm}^{-3}$) plasma.

After the spacecraft has passed the outbound IMB there are some bad data points which need to be checked more carefully with the interactive analysis method (see Appendix A). The electron number density in the magnetosphere seems to be too high (around 1 cm^{-3}) on the inbound, which might be due to the spacecraft having another attitude than during the Saturn Orbit Insertion, when the relationship between n_e and U_{SC} were obtained. Another reason for the higher density could be that the upstream plasma conditions for the T12 flyby are different than for T10 (see also section 5.3).

5.2.3 T8

The T8 flyby occurred on November 28, 2005, with closest approach at 04:15 SCET at an altitude of 1446 km. The encounter geometry was similar to the ones for the T10 and T12 flybys, except that during T8, the spacecraft passed at the exobase level, which is closer to Titan than during T10 and T12 (see Figure 5.8).

The measurements from the T8 flyby are incomplete since the LP was in the wake of the spacecraft during a large part of the passage through the interaction region (see Figure A.3). Since the satellite moves with a high speed ($\sim 6 \text{ km/s}$) compared to the thermal speed of the ions ($\sim 1 \text{ km/s}$), the ions get swept away by the spacecraft motion. As the electrons follow the motion of the ions, the concentration of both ions and electrons will be lower behind the satellite than in the surrounding plasma [4]. This makes it very hard to estimate the correct plasma parameters and the flyby will therefore not be discussed in detail. However, the upper hybrid resonance emissions give a good estimation of the electron number density in the interaction region; $n_e \sim 100 \text{ cm}^{-3}$. This is higher than for the other investigated flybys,

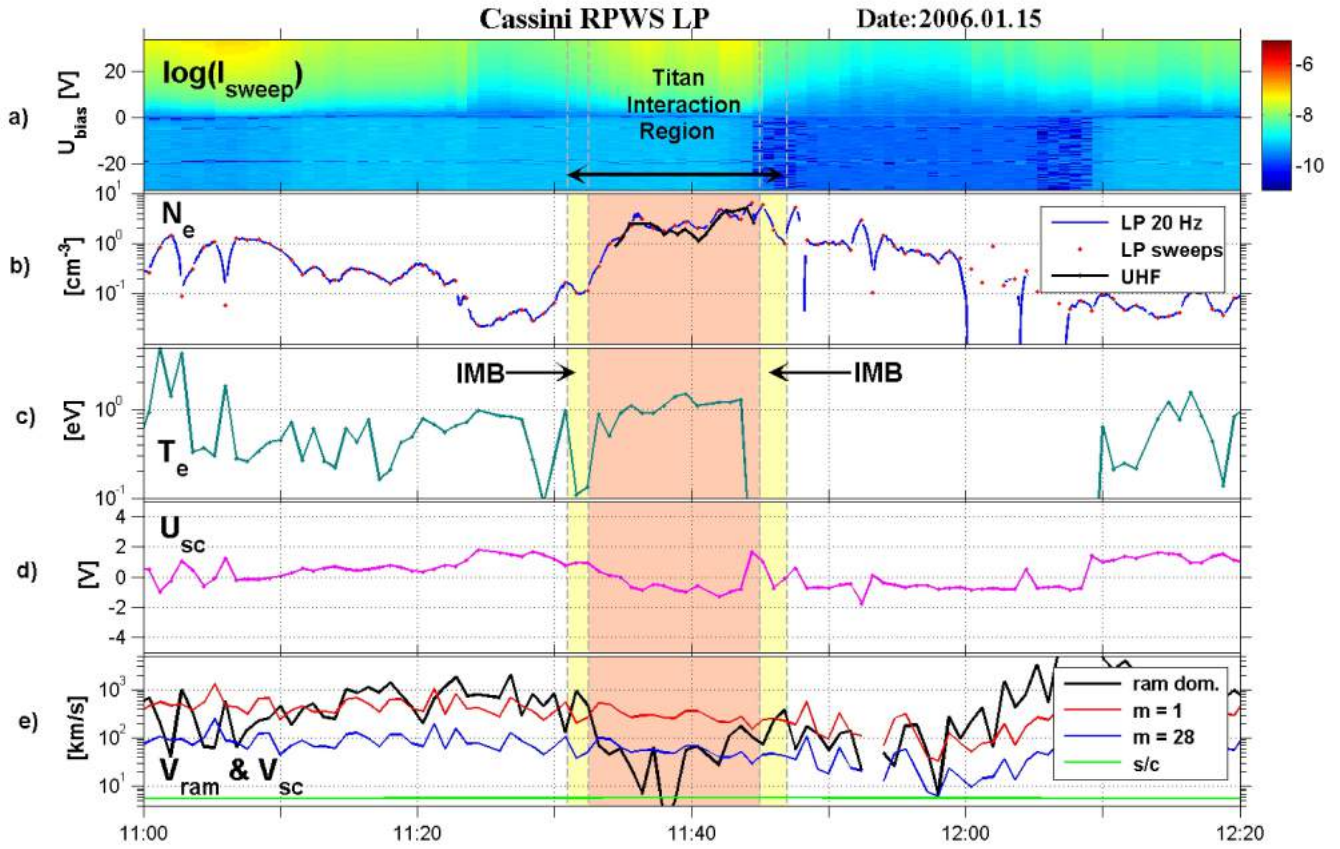


Figure 5.5: Langmuir Probe observations during the T10 flyby. Panel a) shows the calibrated LP measurements. The derived electron number density is shown in panel b). Panel c) presents the electron temperature and panel d) the spacecraft potential. Panel e) provides estimations of the ion ram speed from two different methods; one assuming two different ion masses (red curve and blue curve) and one using the slope from the ion part of the sweep data (black curve).

which is expected as the T8 flyby was deeper in Titan's plasma environment. In this case, the increase in electron density is used as the only criteria to locate the IMB at 04:00 SCET (inbound) and 04:20 SCET (outbound).

5.3 Comparison between the Flybys

As described earlier, the investigated flybys all occurred on the ramside of Titan, and partially in shadow. On the nightside it is evident that electron impact is the dominant ionization process. On the dayside, on the other

hand, it is difficult to predict how much the photoionization contributes to the total ion production. For this reason, the production rates have been calculated along the trajectory of Cassini. Figure 4.9 shows that the photoionization is less important than the electron impact ionization for flyby T10, by approximately a factor 10. The same holds for T12 and T8.

In Figure 5.8 the trajectories of the three flybys are displayed and Figure 5.9 shows comparisons between these flybys. Panel a) and b) present the total production rate of N_2^+ and CH_4^+ due to electron impact and photoionization, respectively. Panel c) shows the total production rate and panel d) the electron number density given by the LP sweep analysis. To be able to compare the flybys, the values have been plotted versus the distance to Titan (in the y direction of Titan's centered reference system) instead of versus time.

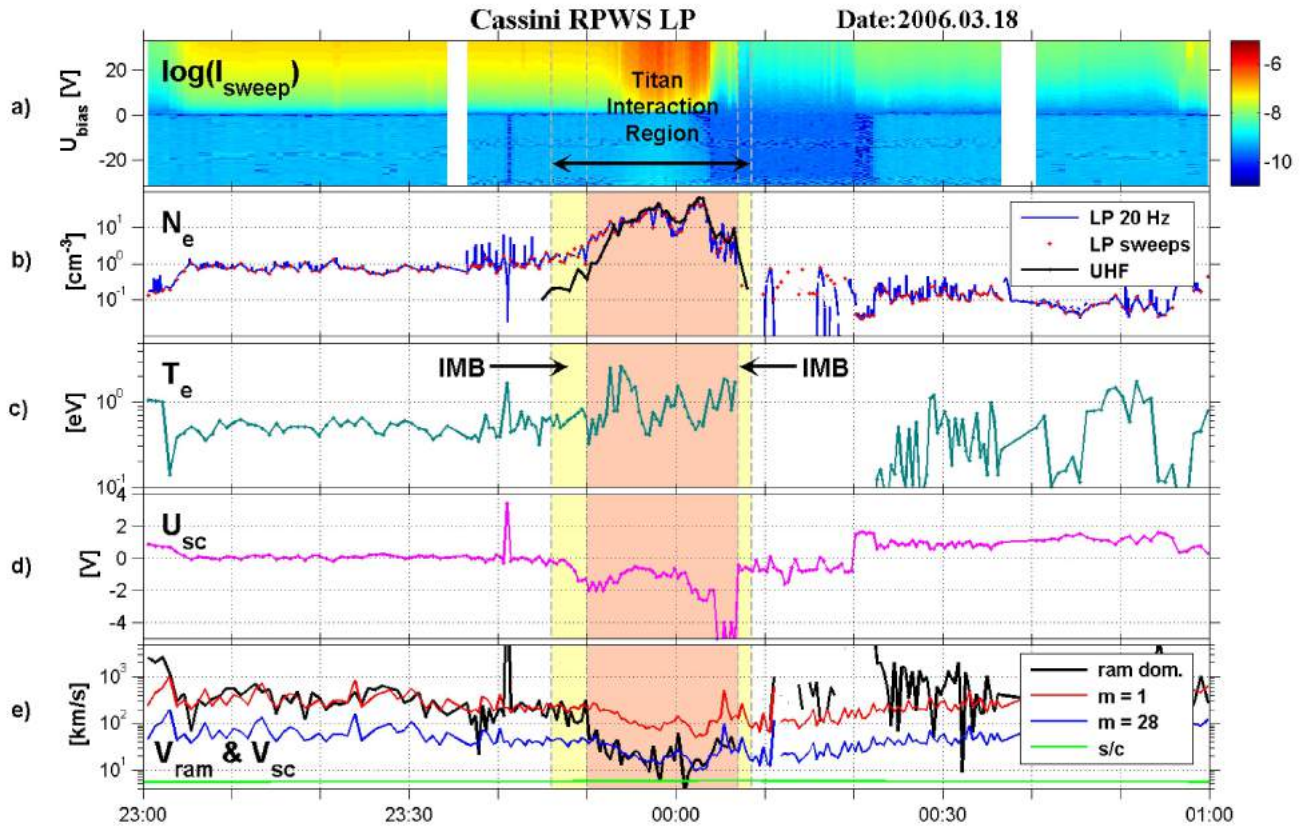


Figure 5.6: Langmuir Probe observations during the T12 flyby. The figure is done in the same way as Figure 5.5.

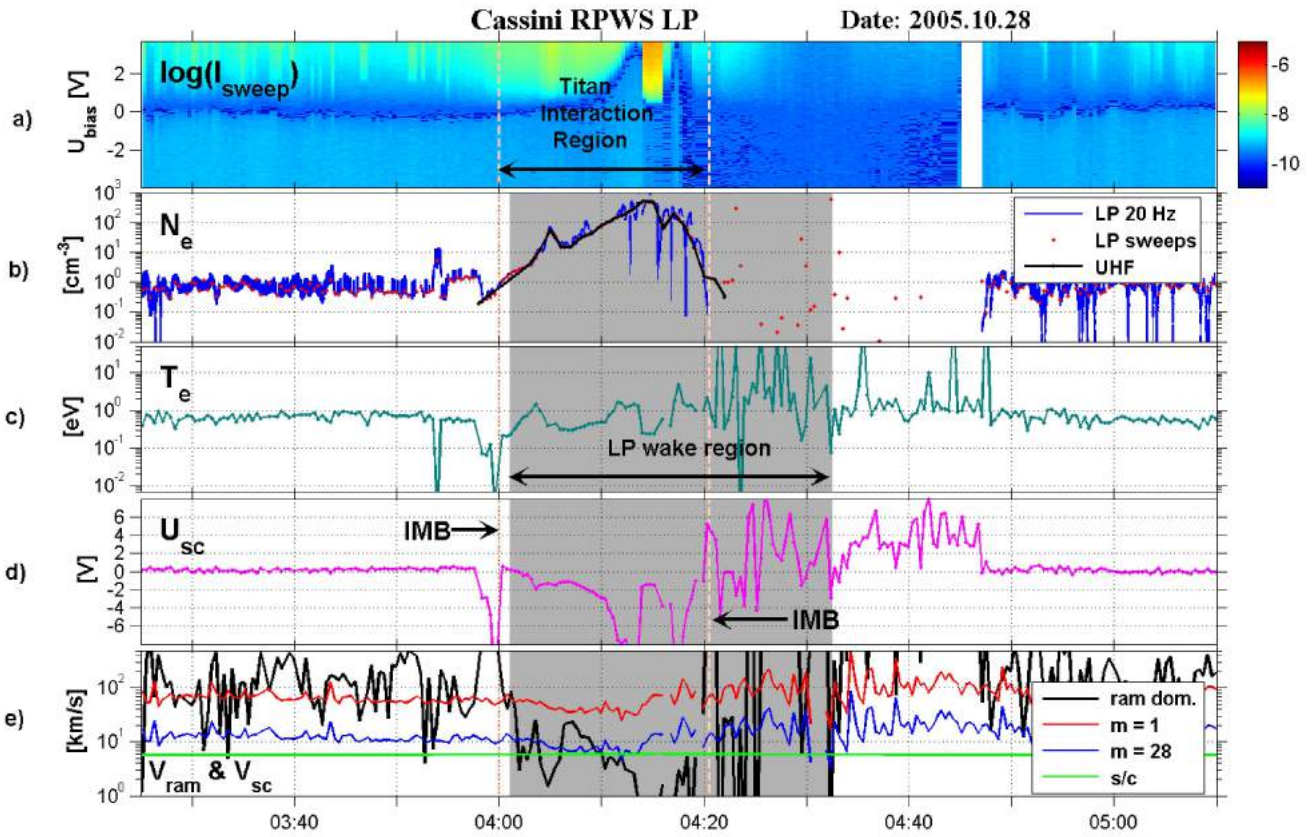


Figure 5.7: Langmuir Probe observations during the T8 flyby. The figure is done in the same way as Figure 5.5.

Panel a) of Figure 5.9 shows that the production rate due to electron impact is very similar for T10 and T12 since the geometry of the two flybys are almost identical. The production rate is more than a factor 1000 higher for T8 due to the lower altitude of that flyby.

From panel b) it is seen that the peak of photoionization is shifted outwards (to the left) for T12 compared with T10. This is an effect of the different SLT for the two flybys; T10 occurred at 08:30 SLT and T12 at 06:25 SLT.

T8 took place at 09:20 SLT and the peak of photoionization is shifted outwards, to about the same distance from Titan than for T10. Again, the reason for this is that the T8 flyby was closer to Titan's exobase than T10, and hence the photoabsorption region was reached earlier.

Panel c) presents the total ion production rate, i.e., the sum of the productions due to electron impact and photoionization. Since photoionization is less important than electron impact ionization in this case, the total pro-

duction rate is almost identical to the one due to electron impact.

The ionization curves are nearly symmetric around the peak production, but the electron number densities seen in panel d), do not show the same behaviour. This asymmetry means that the ion production is not the dominant factor controlling the electron number density. Probably, the dynamics of the plasma affects the behaviour of the electron populations more. To investigate this more thoroughly, a global model for the plasma flow around Titan is needed.

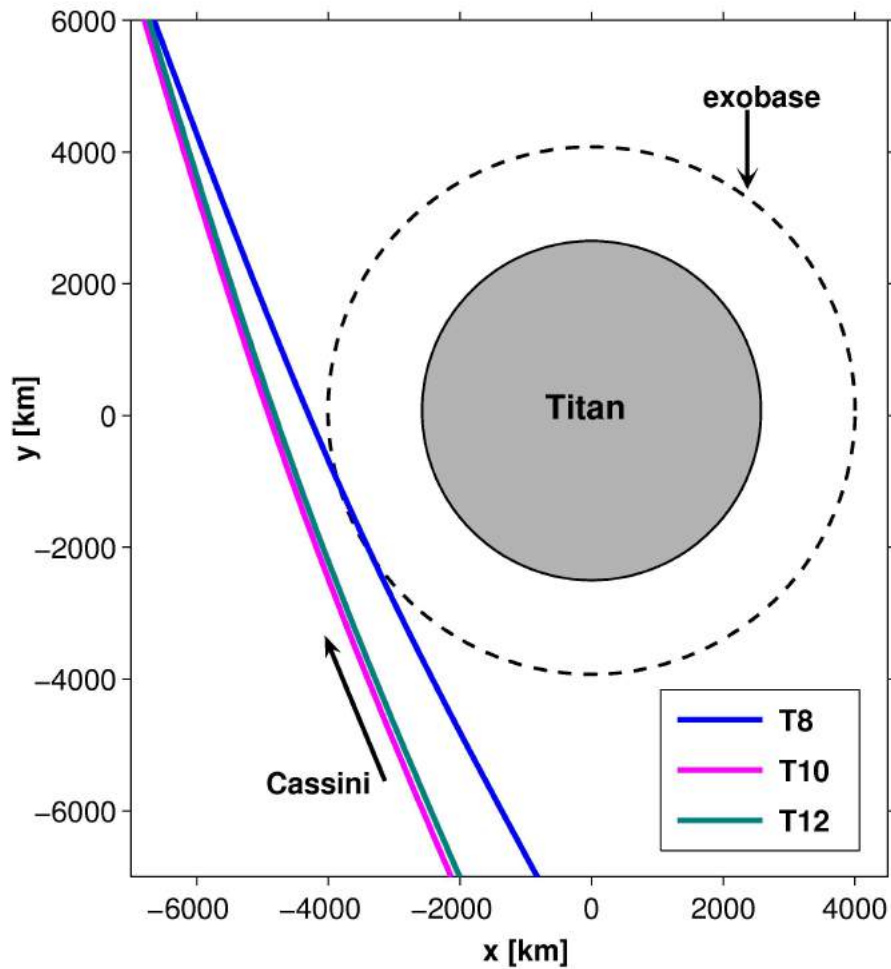


Figure 5.8: The trajectories of Cassini for the investigated flybys. The encounter geometry of T10 and T12 are very similar, while the T8 flyby passed closer to the exobase level than the other two.

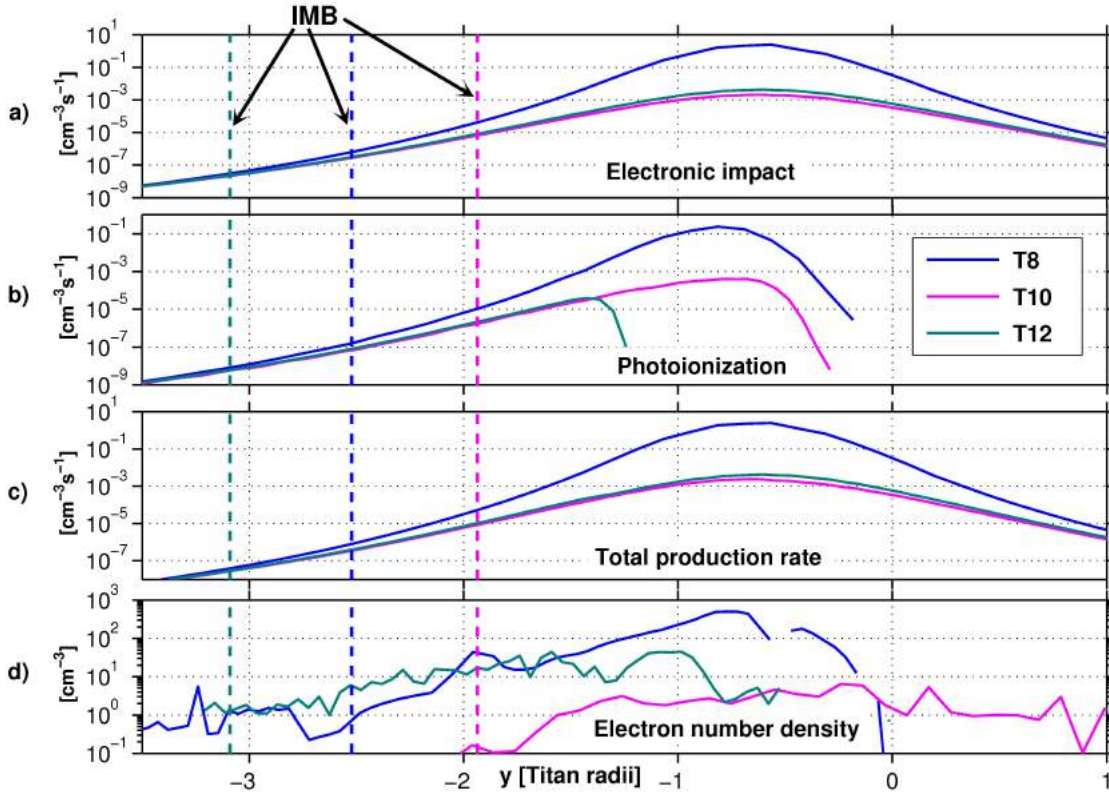


Figure 5.9: Comparison between flybys T8, T10 and T12. Panel a) and b) shows the N_2^+ electron impact and photoionization production rates, respectively, for each flyby. Panel c) shows the sum of these two contributions and panel d) the electron number density. The locations of the inbound IMB are also indicated.

One aim of this study was to investigate if the peak in electron density follows the peak in ion production, i.e., to investigate if more ion production leads to higher electron density and thereby more plasma, which in turn might influence the location of the IMB. For flybys T8 and T10 this seems to hold true; the peak of total ionization coincides with the peak in electron density and the higher production rate during T8 seems to cause the IMB to move further out compared to the T10 flyby.

For T12, on the other hand, the peak in electron density does *not* coincide with the peak in ion production. The locations of the peak production and the IMB are both shifted outwards and the electron density is a factor 10 times higher for T12 compared with T10, although the ion production is the same. One explanation for these differences is that a global simulation model is needed to fully model the plasma behaviour above the exobase since plasma dynamics are of great importance there. The upstream plasma

conditions might also influence the planetary plasma around Titan to a large extent. From Figures 5.5 and 5.6 it is seen that the electron number density in the magnetosphere is $\sim 0.2 \text{ cm}^{-3}$ for T10 and $\sim 1 \text{ cm}^{-3}$ for T12. The higher upstream electron density for T12 is probably connected to a spinning structure in the outer magnetosphere of Saturn, which might influence the plasma environment close to Titan [25].

The main idea of this study was to investigate whether the location of the IMB is sensitive to the Saturn Local Time, i.e., if the orbital phase of Titan influences the interaction region and the location of the boundary. The SLT of a flyby determines from which direction the photons are incident, compared to the direction of the incident electrons, i.e., the angle between the two ionization sources. For the *investigated* flybys, it can be concluded that the location of the IMB is *not* sensitive to the SLT of the flyby, mainly because the photoionization was small compared to the electron impact ionization. If flybys with different encounter geometries were investigated – where the photoionization is of greater importance – it might be found out the location of the IMB is influenced by the SLT.

Chapter 6

Conclusions

Up to now, the Cassini spacecraft has successfully completed several tens of Titan flybys. They have revealed a complex and highly dynamic structure of the plasma environment of Titan. The goal of this study was to improve the understanding of Titan's interaction with the co-rotating plasma of Saturn. In this thesis, the influence of Titan's orbital position on its planetary plasma environment has been investigated. The main focus has been on the ram side Induced Magnetospheric Boundary (IMB) – which is the boundary between the magnetospheric plasma of Saturn and the planetary plasma of Titan – and how this boundary is sensitive to the Saturn Local Time (SLT).

Investigations of the location and structure of the IMB have been performed in two ways: First, a theoretical model of the ion production in Titan's vicinity has been developed. Second, Langmuir Probe data from three Titan flybys has been analysed. Finally, the observations were compared with the model predictions.

6.1 Scientific Results

The main idea of this study was to investigate whether the location of the IMB is sensitive to the SLT. For the investigated flybys it can be concluded that this is *not* the case, mainly because the photoionization was small, compared to the electron impact ionization, and did not influence the ion production much. Looking at flybys with encounter geometries where photoionization is more relevant could still show that the SLT influences the location of the IMB.

Another aim of this study was to examine whether the electron number density is sensitive to the ion production in Titan's interaction region. That is, to investigate if more ion production leads to a higher electron number density and thereby more plasma. That might in turn influence the location of the IMB by moving it further out from Titan. For flybys T8 and T10 these ideas seem to be correct: The peak in ion production coincides

with the peak in electron number density and the higher plasma density in Titan's interaction region during flyby T8 seems to push the IMB further out compared with flyby T10.

For flyby T12, on the other hand, the peak in electron number density does *not* coincide with the peak in ion production and the electron number density is also higher than expected.

The dynamics of the plasma has been neglected in this study and may explain these differences. A global simulation model, taking into account the full dynamics of Titan's plasma environment, is required to completely characterize the plasma behaviour above the exobase level; due to its complexity such a model was not included in this study. Differences in the upstream plasma conditions might also influence the planetary plasma around Titan to a large extent and could be the cause of the higher electron density observed during flyby T12.

The 3D model developed to estimate the photoproduction can be used for all Titan flybys. It is a flexible tool where the SLT can be adjusted as well as the solar EUV photon flux, which is dependent of the solar activity. The 3D model developed to estimate the electron impact production can also be used for all Titan flybys and is valid for electron temperatures between 150 eV and 500 eV, which is the typical range of magnetospheric electrons. A photoelectron current profile can be provided for each Titan flyby, which is a useful way to accurately estimate the plasma speed from the LP data, especially in the photoabsorption region.

The models derived in this study are already applied in other studies: The models for ion production are being used in the work of Karin Ågren with a chemical model for Titan's ionosphere. Also, the model to calculate the photoelectron current along the trajectory of Cassini is used to analyse all Titan flybys.

6.2 Outlook

In order to get more precise information about the location and structure of the IMB, observations from all plasma instruments on Cassini need to be analyzed and combined. Since the direction and strength of Saturn's magnetic field are very likely to influence the IMB, magnetic field data should be included. A transport code needs to be developed and the upstream plasma condition should be taken into account to gain more knowledge about the IMB characteristics. In this study, electron impact production profiles have been implemented in the simplest way, without information about the magnetic field topology. An improvement of the estimated production can be obtained by implementing the draped magnetic field lines around Titan.

Other flyby geometries should also be investigated, for example around 18 SLT on the ram side and in the equatorial plane of Titan, since photoionization is then of maximum relative importance compared to electron impact ionization. Flybys that occur on the ram side but *not* in the equatorial plane would also be interesting to study, since that would help determining which parameters that are of the highest importance for the location of the IMB. Moreover, flybys T19, T21 and T23 occurred at almost the same SLT but with different trajectories. A comparison between the LP observations and the theoretical model predictions, combined with the ionospheric chemistry model developed by Karin Ågren, may provide useful information concerning the ionosphere of Titan and the IMB.

Given the results of this work, from the theoretical model as well as the data analyses, it should not take much effort to extend the study to include more flybys. This would easily provide new valuable and unique results, especially since the Cassini mission is currently in progress and analysis of the collected data has just started. This thesis has enhanced the present understanding of the encounter between the magnetospheric plasma of Saturn and the planetary plasma of Titan.

Appendix A

Langmuir Probe Data Processing

The collected Langmuir Probe (LP) data¹ needs to be prepared before scientific conclusions can be drawn. The following will provide a global description of the data processing procedure (current version; May, 2006), even though some of the steps might be modified in the future. All the MATLAB routines mentioned here are found in the directory `/home/jwe/Matlab/Cassini` on the BRAIN computer at IRFU. The results of the analyses for the T8, T10 and T12 flybys are discussed in section 5.2 and in chapter 6.

A.1 Voltage Sweep Data

After downloading date, time and encounter geometry for the requested flyby from the Cassini RPWS webpage², the first step in the data preparation is to read the stored data from the LP to a file.

A.1.1 SweepMap

The LP performs a voltage sweep every 48th second in the upstream magnetospheric plasma and every 24th second in the vicinity of Titan. A sweep usually takes $\sim 1/2$ second, during which the voltage is varied from -32 V to $+32$ V and the current is sampled 512 times. Sometimes the sweep is twice as long, resulting in a sample of 1024 points, and sometimes the voltage is varied between $+4$ V to -4 V instead. In all cases, the measured current is in the order of a few nA.

The routines needed to calibrate the LP current measurements are found in `/home/jwe/Matlab/Cassini/SweepMap` and the program that needs to be run is called `Run.m`. It is possible to run the script with a specific time

¹The LP data is stored on the server titan.irfu.se

²www-pw.physics.uiowa.edu/plasma-wave/cassini

interval, expressed in seconds, or for a longer period of time, expressed in hours. When a connection to the database³ has been established, the program reads the LP data for all sweeps in the chosen time interval. For each sweep, the bias voltage versus time, $U_B(t)$, and the current versus bias voltage and time, $I(U_B, t)$, are saved in the file `LP_RawData.mat`.

The output of the program is a 2D color map, see upper panel of Figure A.2, where the color shows the magnitude of the probe current for a given time and voltage.

A.1.2 NewSweep

The next step is to fit the data points for each sweep to the theoretical expressions given by equations 5.1 – 5.4 (see section 5.1) to obtain estimations of the plasma parameters n_e , T_e , T_i , v_i and m_i . An estimate of the spacecraft potential, U_{SC} , is also provided by the sweep analysis. The routines are found in `/home/jwe/Matlab/Cassini/NewSweep` and the program that needs to be run is called `Run.m`. Again, the script can be run with a specific time interval or for a longer period of time. It is also possible to use two different modes; automatic or interactive. In the automatic mode, which should only be used in low density regions ($n_e < 5 \text{ cm}^{-3}$), the data points of each sweep are automatically fitted to the theoretical expressions. The LP is well designed to characterize the plasma in dense and cold regions, but the spacecraft potential, U_{SC} , can be used to evaluate the plasma density in low density regions, see section A.3.

When the plasma density is above 5 cm^{-3} , the photoelectron contribution to the current can be identified and removed from the characteristic U-I curve by using the interactive method. The gradient of the current (see Figure A.1) is used to estimate the number of electron populations and their characteristic potential/energy. The characteristic potential for each electron population (U_1 and U_2 in Figure A.1) will be given by the user. In an iterative process, an estimated fit is proposed until the user validates the fit. After validation, the next sweep is examined in the same way.

The plasma parameters for each sweep are saved in the file `LP_Sweep_Data.dat`, which should be renamed to `LP.dat` when the sweep analysis is completed.

A.2 Continuous Data

Between the sweeps, the Langmuir Probe is working in its continuous mode. The current is then sampled at a constant bias voltage of $\sim 10 \text{ V}$ with high resolution – 20 samples per second. This provides measurements of

³ISDAT on titan.irfu.se

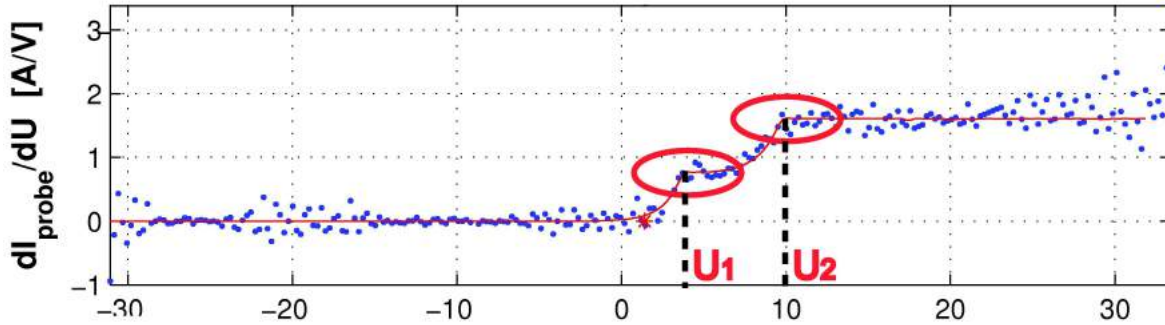


Figure A.1: An example of a LP sweep showing the gradient of the probe current in function of the probe voltage. Two electron populations are identified and their respective characteristic potential, U_1 and U_2 , are initial input suggestions from the user of the interactive method.

$I_e \propto \frac{n_e U_{SC}}{\sqrt{T_e}}$. Between two sweeps, the electron temperature and the spacecraft potential are assumed not to vary significantly. The continuous data can be fitted to the sweep density assuming constant electron temperature and spacecraft potential between two sweeps, thus variations in the high resolution data is caused by density variations [31].

The current and the so called DAC values, which will be used to correct the high resolution density, are obtained by running the script `Run.m` that is found in `/home/jwe/Matlab/Cassini/Density`. The output is saved in the files `LP_Data.dat`, which should be renamed `LP_Ne.dat`, and `LP_DAC.dat`.

A.3 Data Quality Check

In order to get reliable results of the LP analysis, the data needs to be checked to estimate its quality. The spacecraft attitude determines how the LP is located in space and with respect to the incoming solar radiation. The ram direction of the spacecraft determines how the LP is located with respect to the dominating flow direction. The upper hybrid frequency gives an independent estimate of the electron number density in the Titan interaction region.

A.3.1 Spacecraft Attitude

First, the attitude of the spacecraft during the flyby needs to be checked. If there is a change in the attitude, there is probably a change in the photoelectron contribution, and a correction needs to be done (see [20] for more details). The attitude data needs to be downloaded from Terry's Cassini

Utilities webpage⁴.

- Spacecraft attitude data:
Select the appropriate time range, let the time interval be 60 seconds and the attitude type SSQ Spacecraft Axes. Submit and save the information in a file named CASSINI_SA_T#_close.dat where # is replaced by the number of the flyby.

Copy the file, rename it SA_T#.dat and move it to /home/jwe/Matlab/Cassini/Analys where the programs Read_SA.m and Plot_SA.m are used to produce a graph showing the spacecraft attitude during flyby, see Figure A.2.

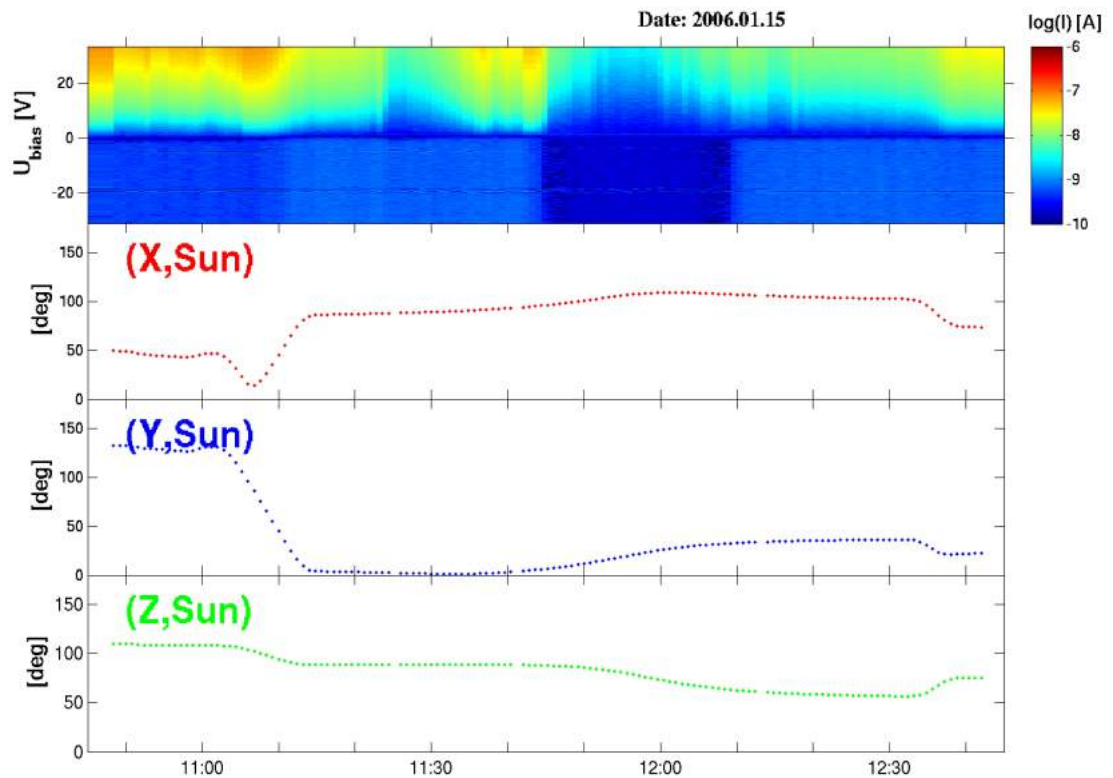


Figure A.2: The upper panel presents the current spectrogram from the T10 flyby. The lower panels show the angle between the solar direction and the X, Y and Z axes. The LP is pointing in the $-X$ direction of the spacecraft coordinate system.

⁴www-pw.physics.uiowa.edu/~tfa/cassatt.html

A.3.2 Ram Direction

Next, the ram direction of the spacecraft with respect to the Langmuir Probe has to be checked. If the LP is in the wake of the spacecraft, the measurements can be strongly affected and the data could be difficult to interpret; this is the case for flyby T8. From the Cassini Ephemeris Tool webpage⁵ the various ephemerides can be downloaded.

- Cassini ephemeris in Saturn equatorial system:
Select the same time range and time interval, choose the origin to be Saturn barycentric, the observer to be Cassini and the coordinate system to be equatorial. Submit and save the information in a file named
`CASSINI_Eph_T#_close.dat`.
- Titan ephemeris in Saturn equatorial system:
Select the same time range and time interval, choose the origin to be Saturn barycentric, the observer to be Titan and the coordinate system to be equatorial. Submit and save the information in a file named
`TITAN_Eph_T#_close.dat`.
- Cassini ephemeris in Titan co-rotational system:
Select the same time range and time interval, choose the origin to be Titan, the observer to be Cassini and the coordinate system to be co-rotational. Submit and save the information in a file named
`CASSINI_Eph_T#_close_Titan_center.dat`.

In the directory `/home/jwe/Matlab/Cassini/Space_Att` the program `Spacecraft_Attitude.m` will generate a graph showing the angle between the LP and the co-rotational direction and the angle between the LP and the ram direction of the spacecraft. This angle to the co-rotational direction needs to be considered outside the IMB (see section 3.2.2 for the definition of the IMB). The angle to the ram direction of the spacecraft needs to be considered inside the IMB. Both these angles should preferably be larger than 50° , since a value close to zero would imply that the LP is in the wake of the spacecraft, see Figure A.3.

A.3.3 Upper Hybrid Frequency

The upper hybrid resonance emission, detected close to Titan by the RPWS antennas, is an electrostatic emission which occurs at the frequency $f_{UHF} \simeq f_p = 8.980 \sqrt{n_e} [\text{kHz}]$ [31]. The electron number density can thus be derived by measuring the frequency of the upper hybrid line, see Figure A.4. Near

⁵www-pw.physics.uiowa.edu/~jbg/cas.html

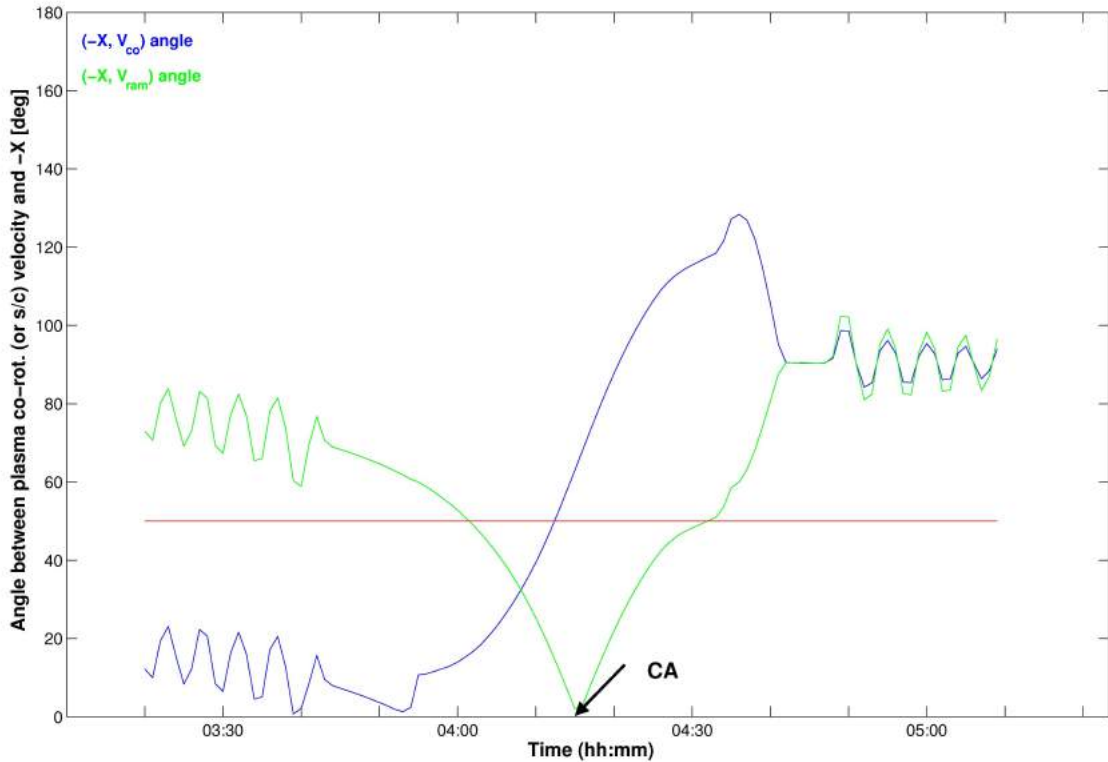


Figure A.3: The result of the ram direction check for the T8 flyby. Around closest approach (CA) the LP is in the wake of the spacecraft, i.e., the angle between the LP and the spacecraft velocity is less than 50° . This is a clear indication that the measurements will be affected and the analysis harder to interpret.

Titan, the result can then be compared with the electron number density given by the LP analysis and thereby provide a complementary validation of the LP density estimation. The upper hybrid resonance data (80 kHz wideband) can be downloaded from the Cassini RPWS Team Webpage⁶.

A.4 Analysis and Plotting

Now, the data is ready to be illustrated with the help of a set of plotting routines. Some more ephemerides needs be downloaded from the Cassini Ephemeris Tool webpage and put into the directory `/home/jwe/Matlab/Cassini/Analys.`

- Cassini ephemeris in Titan geographic system:

⁶cassini.physics.uiowa.edu/cassini/team/team.html

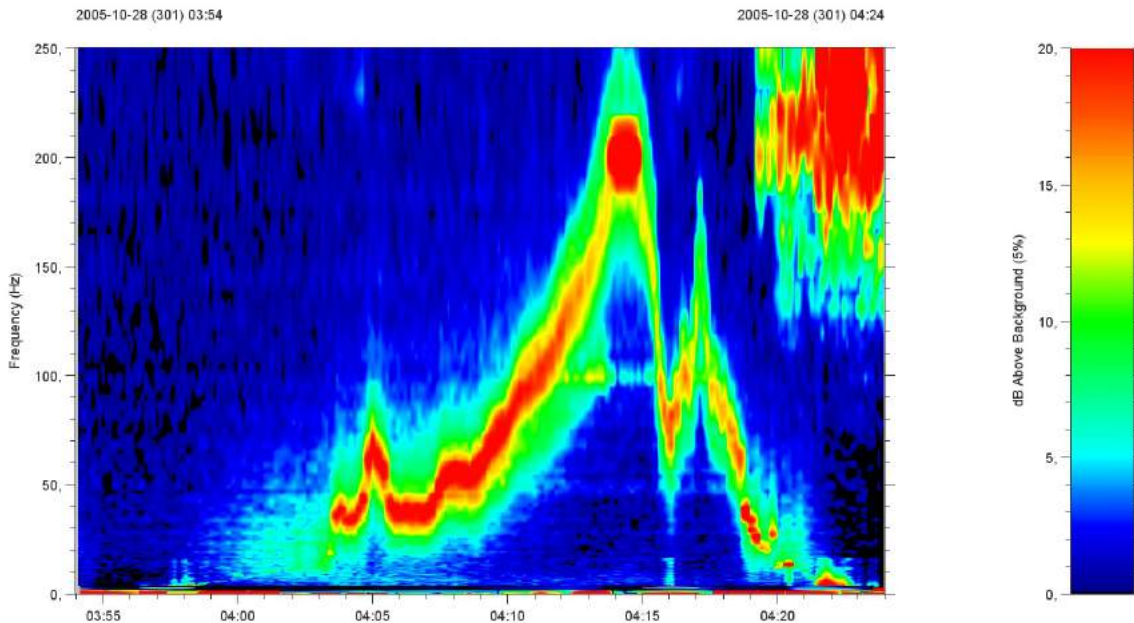


Figure A.4: Plasma wave electric field intensity in the Titan interaction region during the T8 flyby. The upper hybrid resonance line is clearly visible with emissions between 30 kHz and 200 kHz. Since the LP was in the wake during the flyby, the values of n_e derived from f_{UHF} can be used as a reference of the electron number density in the Titan interaction region.

Save the information in a file named `T#_Eph.dat`.

- Cassini ephemeris in Titan ecliptic system:
Save the information in a file named `T#_V.dat`.
- Cassini ephemeris in Saturn ecliptic system:
Save the information in a file named `Eph#_Sat.dat`.
- Cassini ephemeris in Titan co-rotational system:
Save the information in a file named `T#_traj.dat`.

The files `LP_RawData.mat`, `LP.dat`, `LP_Ne.dat` and `SA.T#.dat` should be moved to the same directory as well.

A.4.1 Correction of the Sweep Density in the Outer Magnetosphere

`Read_T#.m` is the main program of the data preparation procedure. After some definitions of constants in the beginning of the script, the plasma parameters from the calibrated sweeps (`LP.dat`) are loaded. Since the LP

measures the total probe current, i.e., the contribution from both the electrons of the plasma and the photoelectrons surrounding the probe, it is hard to determine the electron number density of the plasma. To avoid this problem, an empirical relationship is used to determine the electron number density in regions where $n_e < 5 \text{ cm}^{-3}$. The relationship between the density given by the electron spectrometer of the CAPS instrument and the spacecraft potential determined by the LP during the Saturn Orbit Insertion (SOI) is seen in Figure A.5. The electron number density in the outer magnetosphere is thus corrected using only the spacecraft potential given by the LP. This is done in the function `Correct_Ne.m`.

When the relationship between N_e and U_{SC} was determined, the spacecraft had a constant attitude with respect to the Sun. Recent analysis suggests that the spacecraft potential may be affected by the attitude and that different relations between N_e and U_{SC} might then be needed for different spacecraft attitudes. Further investigations are needed to make a correct estimation of the electron number density possible, independently of the spacecraft attitude with respect to the Sun.

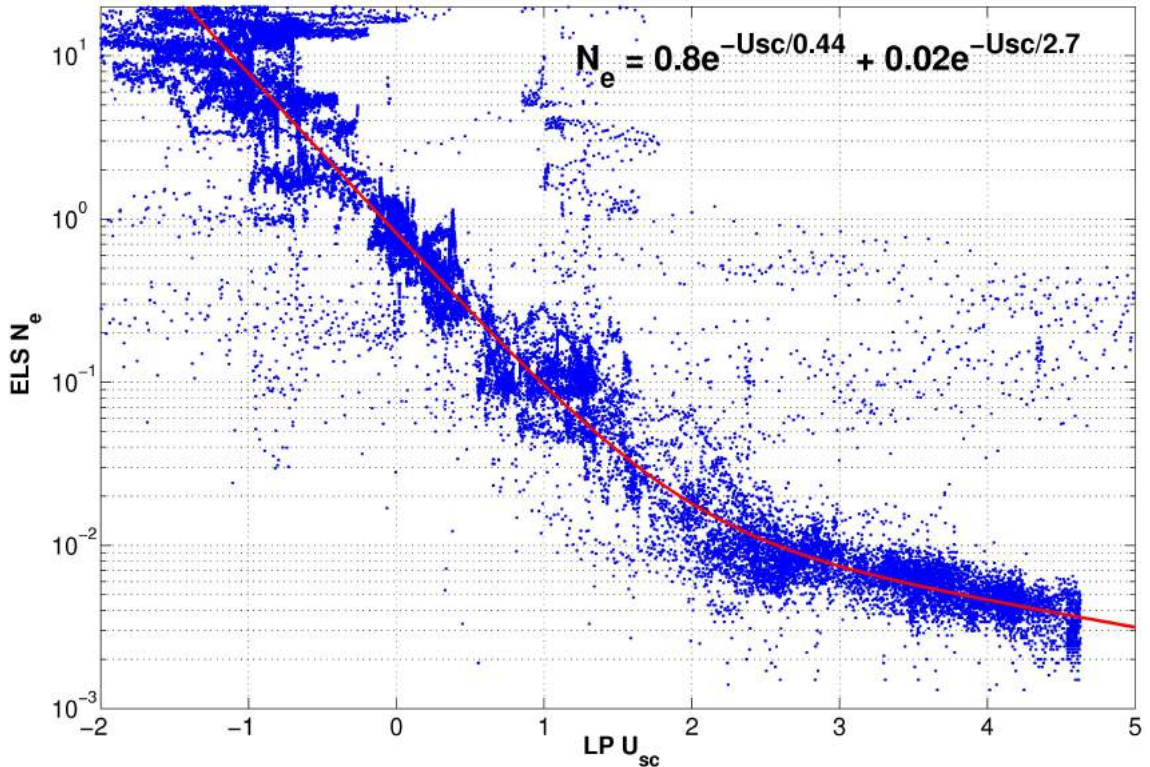


Figure A.5: Empirical relationship between the electron number density and the spacecraft potential used in the outer magnetosphere.

A.4.2 Estimation of the High Resolution Density

The current measurements from the continuous mode (`LP_Ne.dat`) are now loaded. The high resolution density can be estimated from the plasma parameters derived in the previous step, assuming constant electron temperature and spacecraft potential between two sweeps, and by using the relation $I_e \propto \frac{n_e U_{SC}}{\sqrt{T_e}}$. In the function `Correct_20.m` the high resolution energy will be fitted to the sweep density for each point of time where there is a sweep.

A.4.3 Estimation of the Plasma Speed

All the downloaded ephemeris data is now loaded and the velocity of the spacecraft is calculated. There are two independent methods to estimate the ion ram speed of the plasma from the ion current of the LP data [31]. For negative bias voltages, the electron current can be neglected since electrons are repelled; thus the resulting current is the sum of the ion and photoelectron contributions. Assuming that the velocity term (ram term) of the ion current dominates, i.e., $k_B T_i \ll \frac{m_i v_i^2}{2}$, either the slope or the DC level of the ion current can be used to determine the ram speed. If the DC level of the ion current is used, the ion mass needs to be assumed (see section 5.2).

A method of extracting the photoelectron contribution from the ion current by using the instrument yield of the LP and the UV intensity along the spacecraft trajectory has recently been developed, see section 4.5, [39] and [20].

A.4.4 RPWS, CAPS and MAG Data

Data from the Cassini Plasma Spectrometer (CAPS), the Radio and Plasma Wave Science (RPWS) and the Dual Technique Magnetometer (MAG) instruments can be downloaded from the MAPSview webpage⁷ for the investigated flyby. When the data is unzipped and put in the analysis directory, the scripts `Read_CAPS_ISPC.m`, `Read_CAPS_ESPC.m`, `Read_RPWS.m` and `Read_MAG.m` should be read at the end of `Read_T#.m`. This will make it possible to plot the downloaded data together with the LP data.

A.4.5 Plotting Tools

The data can now be plotted in different ways. First, the script `Read_T#.m` should be run to get access to all prepared data.

- `Plot_Main.m` plots the current spectrogram together with estimations of electron number density, electron temperature, spacecraft potential, UV intensity and ion speed.

⁷mapsview.engin.umich.edu

- `Plot_Main_Instrument.m` plots the ion and electron spectrograms from the CAPS instrument, the RPWS wave data and the magnetic field data from the MAG instrument together with the obtained electron density from the LP.
- `T#_traj.m` plots the trajectory of the spacecraft in the Titan centered coordinate system with the electron number density projected along it.
- `Plot_production_trajectory.m` plots the production rates of N_2^+ and CH_4^+ , due to electron impact and photoionization, along the trajectory of the spacecraft. The script also plots UV intensity along the trajectory and 2D maps showing where the ionization takes place for a given Saturn Local Time.

In the directory `/home/jwe/Matlab/Cassini/Analys` there are several more scripts that can be used as an aid to interpret the results of the analysis.

Appendix B

MATLAB Routines

The MATLAB routines that have been developed to model the neutral atmosphere of Titan and the ionization processes that takes place in the ionosphere, are presented here.

Sections B.1 and B.2 contain programs that calculate the neutral densities for the species N_2 and CH_4 , in 1D and 2D respectively. Reference values for the densities and temperatures at certain altitudes are used. The densities are calculated for an altitude of 700 km and above. Below this, investigations have not been performed and little is known about the atmospheric behavior.

The routines in sections B.3 and B.4 are used to determine the production rates of N_2^+ and CH_4^+ by electronic impact. The electronic impact cross sections and electron energies are downloaded, and the temperature of the electrons are assumed to be 200 eV.

The photoionization production rates of N_2^+ and CH_4^+ are calculated in sections B.5 and B.6, using solar EUV flux from the EUVAC Solar Flux Model [32]. Absorption and photoionization cross sections for the two species are also used in the calculations.

The MATLAB routine in section B.7 is used to determine the production rates and the UV intensity along the trajectory of Cassini. Also, 2D maps are produced that show where the two different ionization processes occur, and the location of the trajectory during the flyby.

All programs can be extended to include other particle species and can also be used to investigate other flybys with a similar encounter geometry.

B.1 Neutral_density_1D.m

```

%%%%%%%%%%%%%%%%%%%%%%%%%%%%%%%%%%%%%%%%%%%%%%%%%%%%%%%%%%%%%%%%%%%%%%%%
% Description: This program calculates the neutral density      %
%              profiles in 1D for the species N2 and CH4 in   %
%              Titan's atmosphere.                            %
%                                                            %
% Malin Westerberg, Swedish Institute of Space Physics,     %
% Uppsala, 2006.                                           %
%%%%%%%%%%%%%%%%%%%%%%%%%%%%%%%%%%%%%%%%%%%%%%%%%%%%%%%%%%%%%%%%%%%%%%%%

clear all;
close all;

% Define constants

G      = 6.672e-11; % Gravitational constant, [m^3 s^-2 kg^-1]
k      = 1.38e-23; % Boltzmann constant, [J/K]
e      = 1.602e-19; % Fundamental charge, [C]
u      = 1.66e-27; % Atomic mass constant, [kg]
MT     = 1.34e+23; % Mass of Titan, [kg]
RT     = 2575;    % Radius of Titan, [km]
me     = 9.11e-31; % Electron mass, [kg]
mN2    = 28.013*u; % Mass of N2 molecule, [kg]
mCH4   = 16.043*u; % Mass of CH4 molecule, [kg]
Ne     = 0.1e+6;  % Assumed electron density, [m^-3]
Te     = 200;    % Assumed electron temperature, [eV]

% Temperatures, [K]

T1_N2  = 170.7; % For 700 < r < 1265 km for N2
T2_N2  = 149;   % For r > 1265 km for N2
T2_CH4 = 97.5; % For 925 < r < 1265 km for CH4
T3_CH4 = 149;  % For r > 1265 km for CH4

% Reference altitudes, [km]

H1_N2  = 700;
H2_N2  = 1265;
H2_CH4 = 925;
H3_CH4 = 1265;

% Densities at reference altitudes, [cm^-3]

C1_N2  = 7.2e+11; % For 700 < r < 1265 km for N2
C2_N2  = 2.6e+8;  % For r > 1265 km for N2
C2_CH4 = 6.1e+8;  % For 925 < r < 1265 km for CH4
C3_CH4 = 7.0e+6;  % For r > 1265 km for CH4

% Altitude vectors, [km]

r1 = 700:5:1265;

```


B.2 Neutral_density_2D.m

```

%%%%%%%%%%%%%%%%%%%%%%%%%%%%%%%%%%%%%%%%%%%%%%%%%%%%%%%%%%%%%%%%%%%%%%%%
% Description: This program calculates the neutral density in %
%              2D for the species N2 and CH4 in Titan's %
%              atmosphere. %
% %
% Malin Westerberg, Swedish Institute of Space Physics, %
% Uppsala, 2006. %
%%%%%%%%%%%%%%%%%%%%%%%%%%%%%%%%%%%%%%%%%%%%%%%%%%%%%%%%%%%%%%%%%%%%%%%%

close all;
clear all;

% Define constants

G      = 6.672e-11; % Gravitational constant, [m^3 s^-2 kg^-1]
k      = 1.38e-23; % Boltzmann constant, [J/K]
e      = 1.602e-19; % Fundamental charge, [C]
u      = 1.66e-27; % Atomic mass constant, [kg]
MT     = 1.34e+23; % Mass of Titan, [kg]
RT     = 2575;    % Radius of Titan, [km]
me     = 9.11e-31; % Electron mass, [kg]
mN2    = 28.013*u; % Mass of N2 molecule, [kg]
mCH4   = 16.043*u; % Mass of CH4 molecule, [kg]
Ne     = 0.1e+6;  % Assumed electron density, [m^-3]
Te     = 200;    % Assumed electron temperature, [eV]

% Temperatures, [K]

T1_N2  = 170.7; % For 700 < r < 1265 km for N2
T2_N2  = 149;   % For r > 1265 km for N2
T2_CH4 = 97.5; % For 925 < r < 1265 km for CH4
T3_CH4 = 149;   % For r > 1265 km for CH4

% Reference altitudes, [km]

H1_N2  = 700;
H2_N2  = 1265;
H2_CH4 = 925;
H3_CH4 = 1265;

% Densities at reference altitudes, [cm^-3]

C1_N2  = 7.2e+11; % For 700 < r < 1265 km for N2
C2_N2  = 2.6e+8;  % For r > 1265 km for N2
C2_CH4 = 6.1e+8;  % For 925 < r < 1265 km for CH4
C3_CH4 = 7.0e+6;  % For r > 1265 km for CH4

% Vectors in x and y directions

Δ = 100; % Spatial step

```

```

limit = 4*RT; % Max & min values for x & y

x = -limit:Δ:limit;
y = -limit:Δ:limit;

% Matrix for the radial distance and the density

d = zeros(length(x), length(y));

Nn_N2 = NaN(length(x), length(y));
Nn_CH4 = NaN(length(x), length(y));

% Calculate the distance from the centre of Titan, in [km],
% and the neutral densities, in [cm-3], for all the grid
% points

for i = 1:length(x)
    for j = 1:length(y)

        d(i, j) = sqrt(x(i)^2 + y(j)^2);

        if d(i, j) ≥ (RT + 700) & d(i, j) ≤ (RT + 925)

            Nn_N2(i, j) = C1_N2*exp(((G*MT*mN2)/(k*T1_N2))*...
                (1/(d(i, j)*1000) - ...
                (1/(RT*1000 + H1_N2*1000))));

            Nn_CH4(i, j) = 0.027*Nn_N2(i, j);

        elseif d(i, j) ≥ (RT + 925) & d(i, j) ≤ (RT + 1265)

            Nn_N2(i, j) = C1_N2*exp(((G*MT*mN2)/(k*T1_N2))*...
                (1/(d(i, j)*1000) - ...
                (1/(RT*1000 + H1_N2*1000))));

            Nn_CH4(i, j) = C2_CH4*exp(((G*MT*mCH4)/(k*T2_CH4))*...
                (1/(d(i, j)*1000) - ...
                (1/(RT*1000 + H2_CH4*1000))));

        elseif d(i, j) ≥ (RT + 1265)

            Nn_N2(i, j) = C2_N2*exp(((G*MT*mN2)/(k*T2_N2))*...
                (1/(d(i, j)*1000) - ...
                (1/(RT*1000 + H2_N2*1000))));

            Nn_CH4(i, j) = C3_CH4*exp(((G*MT*mCH4)/(k*T3_CH4))*...
                (1/(d(i, j)*1000) - ...
                (1/(RT*1000 + H3_CH4*1000))));

        end
    end
end

% Save the data in a file

```



```

% Calculate the effective range R as a function of E

R_N2 = 4.3e-7 + 5.39e-6*(energy_N2/1000).^1.67; % [g cm^-2]
R_CH4 = 4.3e-7 + 5.39e-6*(energy_CH4/1000).^1.67;

% Calculate s/R and lambda as functions of E and z

% Empty matrices are created and will be filled with values
% for s/R and lambda for each energy E and each altitude z,
% (s/R and lambda are dimensionless)

s_R_N2 = zeros(length(z) - 1, length(energy_N2));
lambda_N2 = zeros(length(z) - 1, length(energy_N2));

s_R_CH4 = zeros(length(z) - 1, length(energy_CH4));
lambda_CH4 = zeros(length(z) - 1, length(energy_CH4));

for i = 1:length(z) - 1 % i = the row index
    for j = 1:length(energy_N2) % j = the column index for N2

        s_R_N2(i, j) = s_N2(i)/R_N2(j);
        lambda_N2(i, j) = polyval(poly_coeff.2, s_R_N2(i, j));

    end
    for m = 1:length(energy_CH4) % k = the column index for CH4

        s_R_CH4(i, m) = s_CH4(i)/R_CH4(m);
        lambda_CH4(i, m) = polyval(poly_coeff.2, s_R_CH4(i, m));

    end
end

% Find all the places where lambda has negative values and put
% 0's there

index = find(lambda_N2 < 0);
lambda_N2(index) = 0;

clear index

index = find(lambda_CH4 < 0);
lambda_CH4(index) = 0;

%%%%%%%%%%%%%%%%%%%%%%%%%%%%%%%%%%%%%%%%%%%%%%%%%%%%%%%%%%%%%%%%%%%%%%%%
%
% Calculate the production rate by electronic impact for N2
% and CH4.
%
%%%%%%%%%%%%%%%%%%%%%%%%%%%%%%%%%%%%%%%%%%%%%%%%%%%%%%%%%%%%%%%%%%%%%%%%

% Put everything in SI units

Nn_N2 = 1e6*Nn_N2; % Neutral densities, [m^-3]

```

```

Nn_CH4 = 1e6*Nn_CH4;
CS_N2 = 1e-20*CS_N2; % Cross sections, [m^2]
CS_CH4 = 1e-20*CS_CH4;
energy_N2 = e*energy_N2; % Energies, [J]
energy_CH4 = e*energy_CH4;

% Create the integration constants

integral_constant_N2 = Nn_N2(1:(length(Nn_N2) - 1)).*4*...
    Ne*sqrt(1/(2*pi*me))*(1/(e*Te))^(3/2);

integral_constant_CH4 = Nn_CH4(1:(length(Nn_CH4) - 1)).*4*...
    Ne*sqrt(1/(2*pi*me))*(1/(e*Te))^(3/2);

% Create the integrands to use in the integration

integrand_N2 = zeros(length(z) - 1, length(energy_N2));
integrand_CH4 = zeros(length(z) - 1, length(energy_CH4));

for i = 1:length(z) - 1
    for j = 1:length(energy_N2)

        integrand_N2(i, j) = CS_N2(j)*exp(energy_N2(j)/(-e*Te))*...
            energy_N2(j)*lambda_N2(i, j);

    end
    for k = 1:length(energy_CH4)

        integrand_CH4(i, j) = CS_CH4(j)*exp(energy_CH4(j)/...
            (-e*Te))*energy_CH4(j)*...
            lambda_CH4(i, j);

    end
end

% Integrate over all energies E to calculate the production
% rates, [m^-3 s^-1], for each altitude z

q_N2 = zeros(length(z) - 1, 1);
q_CH4 = zeros(length(z) - 1, 1);

for i = 1:length(z) - 1

    q_N2(i) = integral_constant_N2(i)*...
        trapz(energy_N2, integrand_N2(i, :));
    q_CH4(i) = integral_constant_CH4(i)*...
        trapz(energy_CH4, integrand_CH4(i, :));

end

q_N2 = 1e-6*q_N2; % [cm^-3 s^-1]
q_CH4 = 1e-6*q_CH4;

```



```

%%%%%%%%%%%%%%%%%%%%%%%%%%%%%%%%%%%%%%%%%%%%%%%%%%%%%%%%%%%%%%%%%%%%%%%%
%
% Calculate the energy dissipation distribution function as a
% function of the fractional range s/R.
%
%%%%%%%%%%%%%%%%%%%%%%%%%%%%%%%%%%%%%%%%%%%%%%%%%%%%%%%%%%%%%%%%%%%%%%%%

% Make a polynomial curve fitting for the different angular
% dispersions of the incident electron stream

% Unidirectional:

x1_data = [0 0.1 0.2 0.3 0.4 0.5 0.6 0.7 0.8 0.9 1];
y1_data = [0.76 0.98 1.20 1.36 1.44 1.36 1.17 .93 .64 .33 0];

poly_coeff_1 = polyfit(x1_data, y1_data, 9);
s_R = [0:0.01:1];
lambda_1 = polyval(poly_coeff_1, s_R);

% Isotropic (0-70 degrees):

x2_data = [0 0.05 0.1 0.15 0.20 0.25 0.3 0.35 0.4 0.45 0.5...
           0.55 0.6 0.65 0.7 0.75 0.8 0.85 0.9 0.95 1];
y2_data = [1.32 1.5 1.62 1.66 1.6 1.43 1.28 1.15 1.07 0.92...
           0.8 0.68 0.57 0.44 0.37 0.28 0.2 0.13 0.08 0.02 0];

poly_coeff_2 = polyfit(x2_data, y2_data, 9);
s_R = [0:0.01:1];
lambda_2 = polyval(poly_coeff_2, s_R);

%%%%%%%%%%%%%%%%%%%%%%%%%%%%%%%%%%%%%%%%%%%%%%%%%%%%%%%%%%%%%%%%%%%%%%%%
%
% Calculate the atmospheric scattering depth, s.
%
%%%%%%%%%%%%%%%%%%%%%%%%%%%%%%%%%%%%%%%%%%%%%%%%%%%%%%%%%%%%%%%%%%%%%%%%

s_N2 = zeros(length(x) - 1, length(y) - 1);
s_CH4 = zeros(length(x) - 1, length(y) - 1);

% Calculate s as a function of x & y, [s] = g cm^-2

for i = 2:length(x) - 1
    for j = 2:length(y) - 1

        s_N2(i, j) = 1000*mN2*trapz(1e+5*x(1:i), Nn_N2(1:i, j));
        s_CH4(i, j) = 1000*mN2*trapz(1e+5*x(1:i), Nn_CH4(1:i, j));

    end
end

%%%%%%%%%%%%%%%%%%%%%%%%%%%%%%%%%%%%%%%%%%%%%%%%%%%%%%%%%%%%%%%%%%%%%%%%
%
% Calculate the fractional length, s/R, and the energy
% dissipation function, lambda, using the isotropic angular
%
```



```

Nn_N2 = 1e6*Nn_N2; % Neutral densities, [m^-3]
Nn_CH4 = 1e6*Nn_CH4;
CS_N2 = 1e-20*CS_N2; % Cross sections, [m^2]
CS_CH4 = 1e-20*CS_CH4;
energy_N2 = e*energy_N2; % Energies, [J]
energy_CH4 = e*energy_CH4;

% Create the integration constants

integral_constant_N2 = Nn_N2(1:length(x)-1, 1:length(y)-1)*...
    Ne*4*sqrt(1/(2*pi*me))*(1/(e*Te))^(3/2);

integral_constant_CH4 = Nn_CH4(1:length(x)-1,1:length(y)-1)*...
    Ne*4*sqrt(1/(2*pi*me))*...
    (1/(e*Te))^(3/2);

% Create the integrands to use in the integration

integrand_N2 = zeros(length(x) - 1, length(y) - 1,...
    length(energy_N2));

integrand_CH4 = zeros(length(x) - 1, length(y) - 1,...
    length(energy_CH4));

for i = 1:length(x) - 1
    for j = 1:length(y) - 1
        for l = 1:length(energy_N2)

            integrand_N2(i, j, l) = CS_N2(l)*...
                exp(energy_N2(l)/(-e*Te))*...
                energy_N2(l)*lambda_N2(i, j, l);

        end

        for m = 1:length(energy_CH4)

            integrand_CH4(i, j, m) = CS_CH4(m)*...
                exp(energy_CH4(m)/(-e*Te))*...
                energy_CH4(m)*...
                lambda_CH4(i, j, m);

        end
    end
end

% Integrate over all energies E to calculate the production
% rates, [m^-3 s^-1]

q_N2 = zeros(length(x) - 1, length(y) - 1);
q_CH4 = zeros(length(x) - 1, length(y) - 1);

for i = 1:length(x) - 1
    for j = 1:length(y) - 1

```

```

    q_N2(i, j) = integral_constant_N2(i, j)*...
                trapz(energy_N2, integrand_N2(i, j, :));
    q_CH4(i, j) = integral_constant_CH4(i, j)*...
                trapz(energy_CH4, integrand_CH4(i, j, :));

    end
end

q_N2 = 1e-6*q_N2;
q_CH4 = 1e-6*q_CH4;

% Save the data in a file

save Electronic_impact_2D x y Δ limit q_N2 q_CH4;

%%%%%%%%%%%%%%%%%%%%%%%%%%%%%%%%%%%%%%%%%%%%%%%%%%%%%%%%%%%%%%%%%%%%%%%%
%                               End of program                               %
%%%%%%%%%%%%%%%%%%%%%%%%%%%%%%%%%%%%%%%%%%%%%%%%%%%%%%%%%%%%%%%%%%%%%%%%

```

B.5 Photoionization_1D.m

```

%%%%%%%%%%%%%%%%%%%%%%%%%%%%%%%%%%%%%%%%%%%%%%%%%%%%%%%%%%%%%%%%%%%%%%%%
% Description: This program calculates the production rates by %
%              photoionization (with photoabsorbtion) in 1D for %
%              the species N2 and CH4 in Titan's ionosphere for %
%              solar zenith angle = 0.                                     %
%                                                                                   %
% Malin Westerberg, Swedish Institute of Space Physics,                   %
% Uppsala, 2006.                                                           %
%%%%%%%%%%%%%%%%%%%%%%%%%%%%%%%%%%%%%%%%%%%%%%%%%%%%%%%%%%%%%%%%%%%%%%%%

clear all;
close all;

% Define constants

G    = 6.672e-11; % Gravitational constant, [m^3 s^-2 kg^-1]
k    = 1.38e-23; % Boltzmann constant, [J/K]
e    = 1.602e-19; % Fundamental charge, [C]
u    = 1.66e-27; % Atomic mass constant, [kg]
MT   = 1.34e+23; % Mass of Titan, [kg]
RT   = 2575;    % Radius of Titan, [km]
me   = 9.11e-31; % Electron mass, [kg]
mN2  = 28.013*u; % Mass of N2 molecule, [kg]
mCH4 = 16.043*u; % Mass of CH4 molecule, [kg]
Ne   = 0.1e+6;  % Assumed electron density, [m^-3]
Te   = 200;    % Assumed electron temperature, [eV]

% Load data

```



```

load Neutral_density_1D % Contains z, Nn_N2 & Nn_CH4

%%%%%%%%%%%%%%%%%%%%%%%%%%%%%%%%%%%%%%%%%%%%%%%%%%%%%%%%%%%%%%%%%%%%%%%%
%
% Calculate the solar EUV flux using the EUVAC Solar Flux Model.%
%
%%%%%%%%%%%%%%%%%%%%%%%%%%%%%%%%%%%%%%%%%%%%%%%%%%%%%%%%%%%%%%%%%%%%%%%%

% Factor that accounts for solar activity variations

P = 80; % At solar minimum

% Modified reference flux, [cm^-2 s^-1]

F74 = 1e9*[1.2 0.45 4.8 3.1 0.46 0.21 1.679 0.8 6.9 0.965...
           0.65 0.314 0.383 0.29 0.285 0.452 0.72 1.27 0.357...
           0.53 1.59 0.342 0.32 0.36 0.141 0.17 0.26 0.702...
           0.758 1.625 3.537 3 4.4 1.475 3.5 2.1 2.467];

% Scaling factor

A = 1e-3*[10.017 7.125 13.375 19.45 2.775 137.68 26.467 25...
          3.3333 22.45 6.5917 36.542 7.4083 7.4917 20.225...
          8.7583 3.2667 5.1583 3.6583 16.175 3.325 11.8...
          4.2667 3.0417 4.75 3.85 12.808 3.275 4.7667 4.8167...
          5.675 4.9833 3.9417 4.4167 5.1833 5.2833 4.375];

% Wavelength dependent, non-attenuated solar photon flux,
% [cm^-2 s^-1]

I_inf = F74;
%I_inf = F74.*(1 + A*(P - 80)); % Not needed since P = 80

%%%%%%%%%%%%%%%%%%%%%%%%%%%%%%%%%%%%%%%%%%%%%%%%%%%%%%%%%%%%%%%%%%%%%%%%
%
% Calculate the optical depth (tau) as a function of altitude %
% (z) and wavelength (lambda). %
%
%%%%%%%%%%%%%%%%%%%%%%%%%%%%%%%%%%%%%%%%%%%%%%%%%%%%%%%%%%%%%%%%%%%%%%%%

% Wavelength dependent absorption cross section of N2 and CH4,
% [cm^2]; corresponds to wavelengths between 50 - 1050

abs_CS_N2 = 1e-18*[0.72 2.261 4.958 8.392 10.210 10.9 10.493...
                  11.67 11.7 13.857 16.91 16.395 21.675...
                  23.16 23.471 24.501 24.13 22.4 22.787...
                  22.79 23.37 23.339 31.755 26.54 24.662...
                  120.49 14.18 16.487 33.578 16.992 20.249...
                  9.68 2.24 50.988 0 0 0];

abs_CS_CH4 = 1e-18*[0.204 0.593 1.496 2.794 3.857 5.053 4.36...
                   6.033 6.059 7.829 10.165 9.776 14.701...
                   18.77 21.449 24.644 27.924 31.052 30.697...

```

```

33.178 35.276 34.99 39.28 41.069 42.927...
45.458 45.716 46.472 45.921 48.327...
48.968 48.001 41.154 38.192 32.7 30.121...
29.108];

% Calculate the optical depth, dimensionless

tau_N2 = zeros(length(abs_CS_N2), (length(z) - 1));
tau_CH4 = zeros(length(abs_CS_CH4), (length(z) - 1));

for i = 1:length(abs_CS_N2) % i = row index
    for j = 1:(length(z) - 1) % j = column index

        tau_N2(i, j) = abs_CS_N2(i)*trapz(1e+5*...
            z(j:length(z)), Nn_N2(j:length(Nn_N2)));
        tau_CH4(i, j) = abs_CS_CH4(i)*trapz(1e+5*...
            z(j:length(z)), Nn_CH4(j:length(Nn_CH4)));

    end
end

% The total optical depth is the sum of the two components

tau_tot = tau_N2 + tau_CH4;

%%%%%%%%%%%%%%%%%%%%%%%%%%%%%%%%%%%%%%%%%%%%%%%%%%%%%%%%%%%%%%%%%%%%%%%%%%%%%%
%
% Calculate the intensity of the solar photon flux as a function %
% of altitude (z) and wavelength (lambda). %
%
%%%%%%%%%%%%%%%%%%%%%%%%%%%%%%%%%%%%%%%%%%%%%%%%%%%%%%%%%%%%%%%%%%%%%%%%%%%%%%

I_N2 = zeros(length(abs_CS_N2), length(z) - 1);
I_CH4 = zeros(length(abs_CS_CH4), length(z) - 1);

for i = 1:length(abs_CS_N2)
    for j = 1:length(z) - 1

        I_N2(i, j) = I_inf(i)*exp(-tau_tot(i, j)); % [cm^-2 s^-1]
        I_CH4(i, j) = I_inf(i)*exp(-tau_tot(i, j));

    end
end

%%%%%%%%%%%%%%%%%%%%%%%%%%%%%%%%%%%%%%%%%%%%%%%%%%%%%%%%%%%%%%%%%%%%%%%%%%%%%%
%
% Calculate the ion production rate as a function of altitude. %
%
%%%%%%%%%%%%%%%%%%%%%%%%%%%%%%%%%%%%%%%%%%%%%%%%%%%%%%%%%%%%%%%%%%%%%%%%%%%%%%

% Wavelength dependent photoionization cross section of N2 and
% CH4, [cm^2]; corresponds to wavelengths between 50 - 1050

```



```

A = 1e-3*[10.017 7.125 13.375 19.45 2.775 137.68 26.467 25 ...
          3.3333 22.45 6.5917 36.542 7.4083 7.4917 20.225 ...
          8.7583 3.2667 5.1583 3.6583 16.175 3.325 11.8 ...
          4.2667 3.0417 4.75 3.85 12.808 3.275 4.7667 4.8167...
          5.675 4.9833 3.9417 4.4167 5.1833 5.2833 4.375];

% Wavelength dependent, non-attenuated solar photon flux,
% [cm^-2 s^-1]

I_inf = F74;
%I_inf = F74.*(1 + A*(P - 80)); % Not needed since P = 80

%%%%%%%%%%%%%%%%%%%%%%%%%%%%%%%%%%%%%%%%%%%%%%%%%%%%%%%%%%%%%%%%%%%%%%%%
%
% Calculate the optical depth (tau) as a function of altitude
% (z) and wavelength (lambda).
%
%%%%%%%%%%%%%%%%%%%%%%%%%%%%%%%%%%%%%%%%%%%%%%%%%%%%%%%%%%%%%%%%%%%%%%%%

% Wavelength dependent absorption cross section of N2 and CH4,
% [cm^2]; corresponds to wavelengths between 50 - 1050

abs_CS_N2 = 1e-18*[0.72 2.261 4.958 8.392 10.210 10.9 10.493...
                  11.67 11.7 13.857 16.91 16.395 21.675...
                  23.16 23.471 24.501 24.13 22.4 22.787...
                  22.79 23.37 23.339 31.755 26.54 24.662...
                  120.49 14.18 16.487 33.578 16.992 20.249...
                  9.68 2.24 50.988 0 0 0];

abs_CS_CH4 = 1e-18*[0.204 0.593 1.496 2.794 3.857 5.053 4.36...
                   6.033 6.059 7.829 10.165 9.776 14.701...
                   18.77 21.449 24.644 27.924 31.052 30.697...
                   33.178 35.276 34.99 39.28 41.069 42.927...
                   45.458 45.716 46.472 45.921 48.327...
                   48.968 48.001 41.154 38.192 32.7 30.121...
                   29.108];

% Calculate the optical depth, dimensionless

tau_N2 = zeros(length(x) - 1, length(y) - 1, ...
               length(abs_CS_N2));
tau_CH4 = zeros(length(x) - 1, length(y) - 1, ...
               length(abs_CS_CH4));

for i = 2:length(x) - 1
    for j = 2:length(y) - 1
        for l = 1:length(abs_CS_N2)

            chi = atan(y(j)/x(i));

            if x(i) <= 0 % Condition for the dayside

                sec_chi = sqrt(1./(1 - (sqrt(x(i)^2 + y(j)^2)*...
                    sin(chi))./sqrt((transpose(x(1:i)).^2 + ...

```

```

        y(j)^2)).^2));

    tau_N2(i, j, 1) = abs_CS_N2(1)*trapz(1e+5*...
        transpose(x(1:i)), ...
        sec_chi.*Nn_N2(1:i, j));

    tau_CH4(i, j, 1) = abs_CS_CH4(1)*trapz(1e+5*...
        transpose(x(1:i)), ...
        sec_chi.*Nn_CH4(1:i, j));

else % Condition for the nightside

    sec_chi_1 = sqrt(1./(1 - (y(j)./...
        sqrt((transpose(x(1:i)).^2 + ...
        y(j)^2)).^2)));

    sec_chi_2 = sqrt(1./(1 - (sqrt(x(i)^2 + y(j)^2)*...
        sin(chi)./sqrt((transpose(x(1:i)).^2 + ...
        y(j)^2)).^2)));

    tau_N2(i, j, 1) = abs_CS_N2(1)*(2*trapz(1e+5*...
        transpose(x(1:i)), sec_chi_1.*...
        Nn_N2(1:i, j)) - trapz(1e+5*...
        transpose(x(1:i)), sec_chi_2.*...
        Nn_N2(1:i, j)));

    tau_CH4(i, j, 1) = abs_CS_CH4(1)*(2*trapz(1e+5*...
        transpose(x(1:i)), sec_chi_1.*...
        Nn_CH4(1:i, j)) - trapz(1e+5*...
        transpose(x(1:i)), sec_chi_2.*...
        Nn_CH4(1:i, j)));

end
end
end
end

% The total optical depth is the sum of the two components

tau_tot = sum(tau_N2, 3) + sum(tau_CH4, 3);
log_tau_tot = log10(transpose(sum(tau_N2, 3)) + ...
    transpose(sum(tau_CH4, 3)));

%%%%%%%%%%%%%%%%%%%%%%%%%%%%%%%%%%%%%%%%%%%%%%%%%%%%%%%%%%%%%%%%%%%%%%%%%%%%%%
%
% Calculate the intensity of the solar photon flux as a
% function of altitude (h), wavelength (lambda) and solar
% zenith angle (chi).
%
%%%%%%%%%%%%%%%%%%%%%%%%%%%%%%%%%%%%%%%%%%%%%%%%%%%%%%%%%%%%%%%%%%%%%%%%%%%%%%

I = zeros(length(x) - 1, length(y) - 1, length(abs_CS_N2));

for i = 1:length(x) - 1

```

```

for j = 1:length(y) - 1
    for l = 1:length(abs_CS_N2)

        I(i, j, l) = I_inf(l)*exp(-(tau_N2(i, j, l) + ...
                                tau_CH4(i, j, l)));

        % [cm^-2 s^-1]

    end
end
end

I_sum = sum(I, 3);

%%%%%%%%%%%%%%%%%%%%%%%%%%%%%%%%%%%%%%%%%%%%%%%%%%%%%%%%%%%%%%%%%%%%%%%%
%
% Calculate the ion production rate as a function of altitude. %
%
%%%%%%%%%%%%%%%%%%%%%%%%%%%%%%%%%%%%%%%%%%%%%%%%%%%%%%%%%%%%%%%%%%%%%%%%

% Wavelength dependent photoionization cross section of N2 and
% CH4, [cm^2]; corresponds to wavelengths between 50 - 1050

ph_CS_N2 = 1e-18*[0.72 2.261 4.958 8.392 10.210 10.9 10.493...
                11.67 11.7 13.857 16.91 16.395 21.675...
                23.16 23.471 24.501 24.13 22.4 22.787...
                22.79 23.37 23.339 29.235 25.48 15.06 65.8...
                8.5 8.86 14.274 0 0 0 0 0 0 0];

ph_CS_CH4 = 1e-18*[0.204 0.593 1.496 2.794 3.857 5.053 4.36...
                6.033 6.059 7.829 10.165 9.776 14.701...
                18.77 21.449 24.644 27.924 31.052 30.697...
                33.178 35.276 34.99 39.28 41.069 42.927...
                44.8 44.796 44.607 44.693 40.284 25.527...
                13.863 0.136 0.475 0 0 0];

% Ion production rate, [cm^-3 s^-1]

P_N2 = zeros(length(x) - 1, length(y) - 1);
P_CH4 = zeros(length(x) - 1, length(y) - 1);

for i = 1:length(x) - 1
    for j = 1:length(y) - 1

        P_N2(i, j) = Nn_N2(i, j)*sum(permute(I(i, j, :),...
        [1 3 2]).*ph_CS_N2);

        P_CH4(i, j) = Nn_CH4(i, j)*sum(permute(I(i, j, :),...
        [1 3 2]).*ph_CS_CH4);

    end
end
end

```

```

%%%%%%%%%%%%%%%%%%%%%%%%%%%%%%%%%%%%%%%%%%%%%%%%%%%%%%%%%%%%%%%%%%%%%%%%
%
% Rotation of the matrix for the production and photon flux.
%
%%%%%%%%%%%%%%%%%%%%%%%%%%%%%%%%%%%%%%%%%%%%%%%%%%%%%%%%%%%%%%%%%%%%%%%%

% The grid points for the production rates and the photon
% flux need to be rotated to coincide with the direction
% of incoming photons instead of the incoming electrons

% Saturn Local Time for T10

SLT = 8.5; % [h]
angle_SLT = (SLT/24)*2*pi;
angle_ETS = (3*pi/2) - angle_SLT;
% Angle between the incoming electrons and
% the solar direction (Electrons To Solar)

rot_matrix = [cos(angle_ETS) -sin(angle_ETS);...
             sin(angle_ETS) cos(angle_ETS)];

i_center = (length(x) - 1)/2;
j_center = (length(y) - 1)/2;

P_N2_rot = 1e-10*ones(length(x) - 1, length(y) - 1);
P_CH4_rot = 1e-10*ones(length(x) - 1, length(y) - 1);
I_sum_rot = 1e-10*ones(length(x) - 1, length(y) - 1);

for i = 1:length(x) - 1
    for j = 1:length(y) - 1

        index_rot = rot_matrix*[i - (i_center + 1);...
                                j - (j_center + 1)];
        i_rot = fix(index_rot(1) + (i_center + 1));
        j_rot = fix(index_rot(2) + (j_center + 1));
        xa = index_rot(1) + (i_center + 1) - i_rot;
        ya = index_rot(2) + (j_center + 1) - j_rot;
        xf = 1 - xa;
        yf = 1 - ya;
        w1 = xa*ya;
        w2 = xa*yf;
        w3 = xf*ya;
        w4 = xf*yf;

        if ((i_rot >= 1) & (i_rot + 1 <= length(x) - 1)) & ...
            ((j_rot >= 1) & (j_rot + 1 <= length(y) - 1))

            P_N2_rot(i_rot + 1, j_rot + 1) = ...
            P_N2_rot(i_rot + 1, j_rot + 1) + w1*P_N2(i, j);

            P_N2_rot(i_rot + 1, j_rot) = ...
            P_N2_rot(i_rot + 1, j_rot) + w2*P_N2(i, j);

            P_N2_rot(i_rot, j_rot + 1) = ...

```


B.7 Plot_production_trajectory.m

```

%%%%%%%%%%%%%%%%%%%%%%%%%%%%%%%%%%%%%%%%%%%%%%%%%%%%%%%%%%%%%%%%%%%%%%%%
% Description: This program plots the production rates of N2   %
%              and CH4 by photoproduction and electronic impact %
%              as well as the UV factor along the trajectory of %
%              Cassini during a flyby.                          %
%                                                                %
% Malin Westerberg, Swedish Institute of Space Physics,       %
% Uppsala, 2006.                                             %
%%%%%%%%%%%%%%%%%%%%%%%%%%%%%%%%%%%%%%%%%%%%%%%%%%%%%%%%%%%%%%%%%%%%%%%%

close all;
clear all;

RT    = 2575; % Radius of Titan, [km]

%%%%%%%%%%%%%%%%%%%%%%%%%%%%%%%%%%%%%%%%%%%%%%%%%%%%%%%%%%%%%%%%%%%%%%%%
%
% Load the needed data.
%
%%%%%%%%%%%%%%%%%%%%%%%%%%%%%%%%%%%%%%%%%%%%%%%%%%%%%%%%%%%%%%%%%%%%%%%%

load Photoionization_2D_T10;
% Contains: x, y, Δ, limit, I_sum_rot, P_N2_rot, P_CH4_rot

load Electronic_impact_2D;
% Contains: q_N2, q_CH4

P_N2  = P_N2_rot; % Photoionization PR
P_CH4 = P_CH4_rot;
Q_N2  = q_N2; % Electronic impact PR
Q_CH4 = q_CH4;
I_sum = I_sum_rot; % Photon flux/UV intensity

load T10_traj.dat; % Trajectory data

file = T10_traj;
clear T10_traj;

YYYY_traj = file(:, 1);
Day_traj  = file(:, 2);
hh_traj   = file(:, 3);
mm_traj   = file(:, 4);
ss_traj   = file(:, 5);

DATE      = doy2date(YYYY_traj, Day_traj);
MM_traj   = DATE(:, 2);
DD_traj   = DATE(:, 3);

YmdHms_traj = [YYYY_traj MM_traj DD_traj...
               hh_traj mm_traj ss_traj];

```



```

P_CH4_traj(i) = w1*P_CH4(index_x(end)+1, index_y(end)+1)+...
               w2*P_CH4(index_x(end)+1, index_y(end))+...
               w3*P_CH4(index_x(end), index_y(end)+1)+...
               w4*P_CH4(index_x(end), index_y(end));

Q_CH4_traj(i) = w1*Q_CH4(index_x(end)+1, index_y(end)+1)+...
               w2*Q_CH4(index_x(end)+1, index_y(end))+...
               w3*Q_CH4(index_x(end), index_y(end)+1)+...
               w4*Q_CH4(index_x(end), index_y(end));

I_traj(i)      = w1*I_sum(index_x(end)+1, index_y(end)+1)+...
               w2*I_sum(index_x(end)+1, index_y(end))+...
               w3*I_sum(index_x(end), index_y(end)+1)+...
               w4*I_sum(index_x(end), index_y(end));

clear index_x;
clear index_y;

end

%%%%%%%%%%%%%%%%%%%%%%%%%%%%%%%%%%%%%%%%%%%%%%%%%%%%%%%%%%%%%%%%%%%%%%%%%%%%%%
%
% Prepare plotting.
%
%%%%%%%%%%%%%%%%%%%%%%%%%%%%%%%%%%%%%%%%%%%%%%%%%%%%%%%%%%%%%%%%%%%%%%%%%%%%%%

% The location of Titan's surface

theta = (0:360)*2*pi/360;
x_planet = RT*cos(theta);
y_planet = RT*sin(theta);

% Saturn Local Time for T10

SLT = 8.5; % [h]
angle_SLT = (SLT/24)*2*pi;
angle_ETS = (3*pi/2) - angle_SLT;
% Angle between the incoming electrons and
% the solar direction (Electrons To Solar)

% The nightside of Titan

theta_dark = theta/2 + angle_ETS - pi/2;
x_shadow = RT*cos(theta_dark);
y_shadow = RT*sin(theta_dark);

% The 700 km altitude limit

phi = (0:360)*2*pi/360;
x_700 = (RT + 710)*cos(phi);
y_700 = (RT + 710)*sin(phi);

lightgray = [.7 .7 .7];

```

```
% The exobase level

x_exo = (RT + 1429)*cos(phi);
y_exo = (RT + 1429)*sin(phi);

% Time indications

time1 = '\bf 11:30';
time2 = '\bf 12:00';

t_time1 = toepoch([2006 01 15 11 30 00]);
t_time2 = toepoch([2006 01 15 12 00 00]);

% Time interval for plotting

t_start = toepoch([2006 01 15 10 00 00]);
t_end    = toepoch([2006 01 15 13 00 00]);

index_time1 = find(t_traj >= t_time1);
x_time1 = x_traj(index_time1(1));
y_time1 = y_traj(index_time1(1));

index_time2 = find(t_traj >= t_time2);
x_time2 = x_traj(index_time2(1));
y_time2 = y_traj(index_time2(1));

% Find the location of closest approach

[value_CA, index_CA] = min(sqrt(x_traj.^2 + y_traj.^2 + ...
                               z_traj.^2));

x_CA = x_traj(index_CA);
y_CA = y_traj(index_CA);

% Find the places containing NaN's and put very small
% numbers there instead

index_NaN = find(isnan(P_N2_traj));
P_N2_traj(index_NaN) = 1e-15;

clear index_NaN;

index_NaN = find(isnan(Q_N2_traj));
Q_N2_traj(index_NaN) = 1e-15;

clear index_NaN;

index_NaN = find(isnan(P_CH4_traj));
P_CH4_traj(index_NaN) = 1e-15;

clear index_NaN;

index_NaN = find(isnan(Q_CH4_traj));
```

```

Q_CH4_traj(index_NaN) = 1e-15;

%%%%%%%%%%%%%%%%%%%%%%%%%%%%%%%%%%%%%%%%%%%%%%%%%%%%%%%%%%%%%%%%%%%%%%%%
%
% The first figure: Photoionization and electronic impact for
%                   N2 in the ionosphere of Titan and along the
%                   trajectory of Cassini.
%
%%%%%%%%%%%%%%%%%%%%%%%%%%%%%%%%%%%%%%%%%%%%%%%%%%%%%%%%%%%%%%%%%%%%%%%%

f1 = figure;

a1 = subplot(2, 2, 1);
s1 = pcolor(x(1:length(x) - 1), y(1:length(y) - 1), ...
            log10(transpose(P_N2)));
axis 'image';
c_map = colormap(flipud(hot));
shading flat;
hold on;
fill([x_700 x_planet], [y_700 y_planet], lightgray, ...
     'EdgeColor', lightgray);
fill(x_shadow, y_shadow, 'k');
l1 = plot(x_planet, y_planet, 'k', 'LineWidth', 1.5);
l2 = plot(x_700, y_700, 'k--', 'LineWidth', 1);
l3 = plot(x_exo, y_exo, 'k--', 'LineWidth', 1);
l4 = plot(x_traj, y_traj, 'b', 'LineWidth', 1.5);
l5 = plot(x_CA, y_CA, 'k^', 'Markersize', 12);
hold off;
text_1 = text(x_time1, y_time1, time1);
text_2 = text(x_time2, y_time2, time2);
text_3 = text(x_CA - 2000, y_CA, '\bf CA');
c_limit = [-8 2];
set(a1, 'XLim', [-8000 8000], 'YLim', [-8000 8000], ...
     'CLim', c_limit);
set(a1, 'XTick', [-8000 -4000 0 4000 8000], 'TickDir', 'out');

a2 = subplot(2, 2, 2);
s2 = pcolor(x(1:length(x) - 1), y(1:length(y) - 1), ...
            log10(transpose(Q_N2)));
axis 'image';
c_map = colormap(flipud(hot));
shading flat;
hold on;
fill([x_700 x_planet], [y_700 y_planet], lightgray, ...
     'EdgeColor', lightgray);
fill(x_shadow, y_shadow, 'k');
l1 = plot(x_planet, y_planet, 'k', 'LineWidth', 1.5);
l2 = plot(x_700, y_700, 'k--', 'LineWidth', 1);
l3 = plot(x_exo, y_exo, 'k--', 'LineWidth', 1);
l4 = plot(x_traj, y_traj, 'r', 'LineWidth', 1.5);
l5 = plot(x_CA, y_CA, 'k^', 'Markersize', 12);
hold off;
text_1 = text(x_time1, y_time1, time1);
text_2 = text(x_time2, y_time2, time2);

```

```

text_3 = text(x_CA - 2000, y_CA, '\bf CA');
set(a2, 'XLim', [-8000 8000], 'YLim', [-8000 8000],...
      'CLim', c_limit);
set(a2, 'XTick', [-8000 -4000 0 4000 8000], 'TickDir', 'out');
c2_bar = colorbar;
c2_label = text(1.3, 1.05,...
               '\bf log(P_{N2}) [cm^{-3}s^{-1}]',...
               'Units', 'Normalized', 'FontSize', 12);
set(c2_label, 'HorizontalAlignment', 'Center',...
      'VerticalAlignment', 'Middle');
header_text = '\bf Production of N2^+ by photoionization...
              and electronic impact during flyby T10';
header = text(-.35, 1.1, header_text, 'Units', 'Normalized',...
              'FontSize', 14, 'HorizontalAlignment', 'Center',...
              'VerticalAlignment', 'Middle');

a3 = subplot(2, 2, 3);
l1 = plot(t_traj(index), log10(P_N2_traj), 'b',...
          'LineWidth', 2);
hold on;
l2 = plot(t_traj(index), log10(Q_N2_traj), 'r',...
          'LineWidth', 2);
hold off;
grid;
set(a3, 'XLim', [t_start t_end], 'YLim', [-8 -2]);
set(a3, 'YTick', [-8 -7 -6 -5 -4 -3 -2]);
set(a3, 'TickDir', 'out');
ylabel('\bf log(P_{N2}) & log(q_{N2}), [cm^{-3}s^{-1}]');
legend('\bf Photoionization', '\bf Electronic impact');
title('\bf Production of N2^+ along the trajectory');
addtimeaxis(a3);

a4 = subplot(2, 2, 4);
l8 = plot(t_traj(index), log10(I_traj), 'r', 'LineWidth', 2);
grid;
set(a4, 'XLim', [t1 t2]);
set(a4, 'YLim', [7 9]);
set(a4, 'TickDir', 'out');
ylabel('\bf log(I) [cm^{-2}s^{-1}]');
title('\bf UV intensity along the trajectory');
addtimeaxis(a4);

%%%%%%%%%%%%%%%%%%%%%%%%%%%%%%%%%%%%%%%%%%%%%%%%%%%%%%%%%%%%%%%%%%%%%%%%
%
% The second figure: Photoionization and electronic impact for
%                   CH4 in the ionosphere of Titan and along
%                   the trajectory of Cassini.
%
%%%%%%%%%%%%%%%%%%%%%%%%%%%%%%%%%%%%%%%%%%%%%%%%%%%%%%%%%%%%%%%%%%%%%%%%

f2 = figure;

a1 = subplot(2, 2, 1);
s1 = pcolor(x(1:length(x) - 1), y(1:length(y) - 1), ...

```

```

        log10(transpose(P_CH4)));
axis 'image';
c_map = colormap(flipud(hot));
shading flat;
hold on;
fill([x_700 x_planet], [y_700 y_planet], lightgray,...
     'EdgeColor', lightgray);
fill(x_shadow, y_shadow, 'k');
l1 = plot(x_planet, y_planet, 'k', 'LineWidth', 1.5);
l2 = plot(x_700, y_700, 'k—', 'LineWidth', 1);
l3 = plot(x_exo, y_exo, 'k—', 'LineWidth', 1);
l4 = plot(x_traj, y_traj, 'b', 'LineWidth', 1.5);
l5 = plot(x_CA, y_CA, 'k^', 'Markersize', 12);
hold off;
text_1 = text(x_time1, y_time1, time1);
text_2 = text(x_time2, y_time2, time2);
text_3 = text(x_CA - 2000, y_CA, '\bf CA');
c_limit = [-8 2];
set(a1, 'XLim', [-8000 8000], 'YLim', [-8000 8000]);
set(a1, 'XTick', [-8000 -4000 0 4000 8000]);
set(a1, 'CLim', c_limit, 'TickDir', 'out');

a2 = subplot(2, 2, 2);
s2 = pcolor(x(1:length(x) - 1), y(1:length(y) - 1),...
           log10(transpose(Q_CH4)));
axis 'image'
c_map = colormap(flipud(hot));
shading flat;
hold on;
fill([x_700 x_planet], [y_700 y_planet], lightgray,...
     'EdgeColor', lightgray);
fill(x_shadow, y_shadow, 'k');
l1 = plot(x_planet, y_planet, 'k', 'LineWidth', 1.5);
l2 = plot(x_700, y_700, 'k—', 'LineWidth', 1);
l3 = plot(x_exo, y_exo, 'k—', 'LineWidth', 1);
l4 = plot(x_traj, y_traj, 'g', 'LineWidth', 1.5);
l5 = plot(x_CA, y_CA, 'k^', 'Markersize', 10);
hold off;
text_1 = text(x_time1, y_time1, time1);
text_2 = text(x_time2, y_time2, time2);
text_3 = text(x_CA - 2000, y_CA, '\bf CA');
set(a2, 'XLim', [-8000 8000], 'YLim', [-8000 8000]);
set(a2, 'XTick', [-8000 -4000 0 4000 8000]);
set(a2, 'CLim', c_limit, 'TickDir', 'out');
c2_bar = colorbar;
c2_label = text(1.3, 1.05,...
               '\bf log(P-CH4) [cm-3s-1]',...
               'Units', 'Normalized');
set(c2_label, 'HorizontalAlignment', 'Center',...
            'VerticalAlignment', 'Middle',...
            'FontSize', 12);
header_text = '\bf Production of CH4+ by photoionization...
              and electronic impact during flyby T10';
header = text(-.35, 1.1, header_text, 'Units', 'Normalized',...

```


Acknowledgements

First of all I would like to thank my supervisor Ronan Modolo for all his invaluable help during my time at the Swedish Institute of Space Physics. I am thankful to him for guiding me through my work, for always finding time to answer my questions and for helping me tackle problems that have arisen along the way. I would also like to thank Jan-Erik Wahlund for introducing me to the subject and for reading and commenting on the final report.

I am very grateful to Mikael Lundberg for all the help and support he has given me every day. I especially thank him for teaching me MATLAB, for helping me with all kind of computer problems and for making me laugh every day!

I also thank all the personnel at IRF-U for making me really enjoy my time here and particularly Anita Kullen for letting me share her room and for proofreading my report.

Last but not least I want to acknowledge all my fellow master thesis students for the time we have spent together.

Bibliography

- [1] N. Achilleos *et al.*, *Orientation, location and velocity of Saturn's bow shock: Initial results from the Cassini spacecraft*, Journal of Geophysical Research, Vol. 111, Issue A3, 2006.
- [2] K. Beatty, *The New Solar System*, Sky Publishing, 1999.
- [3] H. Backes *et al.*, *Titan's Magnetic Field Signature during the first Cassini Encounter*, Science, Vol. 308, Issue 5724, p. 992–995, 2005.
- [4] R. Behlke *et al.*, *Langmuir Probes*, contributed chapter in *Sensors and Instruments for Space Exploration*, Kiruna, 2000.
- [5] C. Bertucci *et al.*, *Magnetic field draping enhancement at the Martian magnetic pileup boundary from Mars global surveyor observations*, Geophysical Research Letters, Vol. 30, Issue 2, p. 71 ff., 2003.
- [6] C. Bertucci *et al.*, *Magnetic field draping enhancement at Venus: Evidence for a magnetic pileup boundary*, Geophysical Research Letters, Vol. 30, Issue 17, 2003.
- [7] L. Brace *et al.*, *Solar EUV Measurements at Venus based on Photoelectron emission from the Pioneer Venus Langmuir Probe*, Journal of Geophysical Research, Vol. 93, No. A7, 1988.
- [8] T. Cravens *et al.*, *Electron Impact Ionization in the Vicinity of Comets*, Journal of Geophysical Research, Vol. 92, No. A7, 1987.
- [9] T. Cravens *et al.*, *Titan's ionosphere: Model comparison with Cassini Ta data*, Geophysical Research Letters, Vol. 32, Issue 12, 2005.
- [10] C. Elachi *et al.*, *Cassini Radar views the Surface of Titan*, Science, Vol. 308, Issue 5724, p. 970–974, 2005.
- [11] U. Fahlson, *Theory of Electric Field Measurements conducted in the Magnetosphere with Electric Probes*, Space Science Reviews, Vol. 7, p. 238, 1967.

-
- [12] F. Flasar *et al.*, *Titan's Atmospheric Temperatures, Winds and Composition*, Science, Vol. 308, Issue 5724, p. 975–978, 2005.
- [13] M. Fulchignoni *et al.*, *In situ measurements of the physical characteristics of Titan's environment*, Nature, Vol. 438, Issue 7069, p. 785–791, 2005.
- [14] R. Freedman, W. Kaufmann, *Universe*, W. H. Freeman and Company, 2002.
- [15] L. Gan *et al.*, *Electrons in the Ionosphere of Titan*, Journal of Geophysical Research, Vol. 97, No. A8, 1992.
- [16] R. Hartle *et al.*, *Preliminary interpretation of Titan's plasma interaction as observed by the Cassini Plasma Spectrometer: Comparison with Voyager 1*, Geophysical Research Letters, Vol. 33, Issue 8, 2006.
- [17] C. Keller *et al.*, *One-dimensional multispecies magnetohydrodynamic models of the ramside ionosphere of Titan*, Journal of Geophysical Research, Vol. 99, No. A4, p. 6527–6536, 1994.
- [18] M. Kivelson, C. Russel, *Introduction to Space Physics*, Cambridge University Press, 1995.
- [19] J. P. Lebreton *et al.*, *An overview of the descent and landing of the Huygens probe on Titan*, Nature, Vol. 438, Issue 7069, p. 758–764, 2005.
- [20] M. Lundberg, *Investigation of E-ring interaction with Saturn's Inner Magnetosphere, from the Langmuir Probe observations*, Swedish Institute of Space Physics, Uppsala, 2007.
- [21] R. Lundin *et al.*, *Solar Wind-Induced Atmospheric Erosion at Mars: First Results from ASPERA-3 on Mars Express*, Science, Vol. 302, Issue 5692, p. 1933–1936, 2004.
- [22] Y. Ma *et al.*, *Comparison between MHD model calculations and observations of Cassini flybys of Titan*, Journal of Geophysical Research, Vol. 111, Issue. A5, 2006.
- [23] P. Mahaffy *et al.*, *Intensive Titan Exploration Begins*, Science, Vol. 308, Issue 5724, p. 969–970, 2005.
- [24] R. Modolo, G. M. Chanteur *The Kronian Plasma Interaction with Titan from Global Hybrid Simulation*, Journal of Geophysical Research, 2007.
- [25] M. Morooka *et al.*, *Corotating plasma outflow in the outer magnetosphere of Saturn*, Swedish Institute of Space Physics, Uppsala, 2007.

- [26] N. Ness *et al.*, *The Induced Magnetosphere of Titan*, Journal of Geophysical Research, Vol. 87, No. A3, 1982.
- [27] F. Neubauer *et al.*, *Titan's Magnetospheric Interaction*, ESA, Symposium on Titan, p. 267–272, 1999.
- [28] C. Nordling, J. Österman, *Physics Handbook for Science and Engineering*, Studentlitteratur, 1999.
- [29] M. Rees, *Auroral Ionization and Excitation by Incident Energetic Electrons*, Planetary Space Science, Vol. 11, p. 1209–1218, 1963.
- [30] M. Rees, *Physics and Chemistry of the Upper Atmosphere*, Cambridge University Press, 1989.
- [31] R. Modolo *et al.*, *The far plasma wake of Titan from the RPWS observations – a case study*, Swedish Institute of Space Physics, 2007.
- [32] R. Schunk, A. Nagy, *Ionospheres: Physics, Plasma Physics, and Chemistry*, Cambridge University Press, 2000.
- [33] D. Shemansy *et al.*, *The Cassini UVIS Stellar Probe of the Titan Atmosphere*, Science, Vol. 308, Issue 5724, p. 978–982, 2005.
- [34] E. Sittler *et al.*, *Titan interaction with Saturn's magnetosphere: Voyager 1 results revisited*, Journal of Geophysical Research, Vol. 110, Issue. A9, 2005.
- [35] K. Szego *et al.*, *The global plasma environment of Titan as observed by Cassini Plasma Spectrometer during the first two close encounters with Titan*, Geophysical Research Letters, Vol. 32, Issue 20, 2005.
- [36] D. Toublanc *et al.*, *Erratum: Photochemical modeling of Titan's Atmosphere*, Icarus, Vol. 117, p. 218, 1995.
- [37] J.-E. Wahlund *et al.*, *Cassini Measurements of Cold Plasma in the Ionosphere of Titan*, Science, Vol. 308, Issue 5724, p. 986–989, 2005.
- [38] H. Waite *et al.*, *Ion Neutral Mass Spectrometer Results from the First Flyby of Titan*, Science, Vol. 308, Issue 5724, p. 982–986, 2005.
- [39] E. Winkler, *Plasma Densities and Satellite Potentials*, Swedish Institute of Space Physics, Uppsala, 2007.